Computers and Chemical Engineering 116 (2018) 156–175

Contents lists available at ScienceDirect

Computers and Chemical Engineering

journal homepage: www.elsevier.com/locate/compchemeng

Elucidating and handling effects of valve-induced nonlinearities in industrial feedback control loops

Helen Durand[a], Robert Parker[a], Anas Alanqar[a], Panagiotis D. Christofides[a,b,*]

[a] Department of Chemical and Biomolecular Engineering, University of California, Los Angeles, CA 90095-1592, USA
[b] Department of Electrical Engineering, University of California, Los Angeles, CA 90095-1592, USA

ARTICLE INFO

Article history:
Received 23 March 2017
Revised 30 June 2017
Accepted 18 August 2017
Available online 24 August 2017

Keywords:
Model predictive control
Valve dynamics
Chemical processes
Process control
Stiction
Empirical modeling

ABSTRACT

In this work, we investigate the effects of various types of valve behavior (e.g., linear valve dynamics and stiction) on the effectiveness of process control in a unified framework based on systems of nonlinear ordinary differential equations that characterize the dynamics of closed-loop systems including the process, valve, and controller dynamics. By analyzing the resulting dynamic models, we demonstrate that the responses of the valve output and process states when valve behavior cannot be neglected (e.g., stiction-induced oscillations in measured process outputs) are closed-loop effects that can be difficult to predict *a priori* due to the coupled and typically nonlinear dynamics of the process-valve model. Subsequently, we discuss the implications of this closed-loop perspective on the effects of valve dynamics in closed-loop systems for understanding valve behavior compensation techniques and developing new ones. We conclude that model-based feedback control designs that can account for process and valve constraints and dynamics provide a systematic method for handling the multivariable interactions in a process-valve system, where the models in such control designs can come either from first-principles or empirical modeling techniques. The analysis also demonstrates the necessity of accounting for valve behavior when designing a control system due to the potentially different consequences under various control methodologies of having different types of valve behavior in the loop. Throughout the work, a level control example and a continuous stirred tank reactor example are used to illustrate the developments.

1. Introduction

Valves do not respond instantaneously to control signal changes (i.e., their response has dynamics) because they have mechanical parts that move when the control signal changes. Typically, the chemical process control literature assumes that the valve dynamics are so fast that they can be neglected, meaning that the valve output is assumed to immediately equal the value requested by the controller. However, in industry, various valve behaviors are observed that impact control loop performance, though an engineer entering industry after completing his or her undergraduate education typically has had limited exposure to valve behavior. Undergraduate process control courses often handle valve dynamics with linear transfer function models; such dynamics can be related to, for example, resistance of the gas used to apply pressure in a pneumatic actuator to flow at the top of a valve (Coughanowr and LeBlanc, 2009). Valve characteristics (e.g., linear, equal percentage, and square root) may also be reviewed in undergraduate coursework to provide undergraduates with fundamentals regarding valve sizing and the effects of installing a valve on the valve's flow characteristics (the manner in which the flow through the valve is related to the valve opening) (Coughanowr and LeBlanc, 2009; Ogunnaike and Ray, 1994; Riggs, 1999). Though there may be some discussion of other types of valve behavior described by nonlinear models (e.g., saturation of the valve output at its maximum value, failure of a valve to respond to changes in the control signal to the valve for some time after a valve movement direction change due to mechanical parts in a valve (deadband due to backlash) (Choudhury et al., 2005), or stiction (Brásio et al., 2014; Armstrong-Hélouvry et al., 1994), which refers to valve behavior due to friction that can be described by nonlinear dynamic equations), time constraints in a semester/quarter and also a general focus in undergraduate process control on linear dynamic systems do not typically permit an in-depth treatment of nonlinear valve behavior and its impact on process control from a first-principles perspective. However, at chemical plants throughout the world, valve issues such as stiction, deadband, saturation, hysteresis, and

* Corresponding author at: Department of Chemical and Biomolecular Engineering, University of California, Los Angeles, CA 90095-1592, USA.
E-mail address: pdc@seas.ucla.edu (P.D. Christofides).

https://doi.org/10.1016/j.compchemeng.2017.08.008
0098-1354/

deadzone prevent adequate set-point tracking (Jelali and Huang, 2010; Choudhury et al., 2008). Therefore, it would be beneficial if the various types of valve behavior were presented within a single framework so that undergraduates could learn the mathematical structure needed to allow them to understand and compensate for any valve behavior that they encounter in their courses and their careers.

The traditional manner of handling valve behavior, in which various types of valve behavior are treated separately rather than within a single framework, is prevalent in the literature. For example, Durand et al. (2014) demonstrates that even linear valve dynamics can be problematic for a process operated under an optimization-based control design called economic model predictive control (EMPC) (Ellis et al., 2014a; Heidarinejad et al., 2012; Amrit et al., 2011; Rawlings et al., 2012; Huang et al., 2012) when the valve dynamics are neglected in the model utilized by the EMPC for making state predictions; therefore, that work suggests incorporating the valve dynamics in the dynamic process model for the controller. Choudhury et al. (2008) analyzes the range of valve travel over which linear control design theory would be expected to be adequate when a process that can be effectively modeled with a linear model receives a flow rate from a valve with a square root or an equal percentage inherent valve characteristic. Zabiri and Samyudia (2006) develops an MPC-based method for linear processes where the valve is subject to backlash. The literature analyzing and compensating for the stiction nonlinearity is particularly extensive, with reviews such as Brásio et al. (2014) categorizing the methods, though stiction compensation remains an important research topic with newer works such as those in Durand and Christofides (2016), Bacci di Capaci et al. (2017) and Munaro et al. (2016) expanding the compensation literature.

Another feature of the valve behavior literature is that the types of processes and control laws handled are often limited. For example, despite the recognition in (Thornhill and Horch, 2007; Jelali and Huang, 2010; Choudhury et al., 2005) that the controller, process, and valve dynamics all play a role in determining the trajectories of the measured outputs of a closed-loop system with a sticky valve, a summary table in Thornhill and Horch (2007) focuses on combinations of linear processes (integrating and non-integrating) and linear controllers (proportional (P) and proportional-integral (PI)) with different stiction characteristics for a valve in the control loop to clarify which combinations are expected to result in limit cycling of the valve output. This is consistent with much of the stiction compensation literature, which is developed assuming linear process models and linear controllers. Furthermore, the stiction literature generally focuses on single-input/single-output control loops. It is widely appreciated, however, that chemical processes are typically described by nonlinear dynamic models with multiple inputs.

Motivated by these considerations, the primary contribution of this work is the development of a single, comprehensive systems engineering framework for understanding the impacts of various types of valve behavior on closed-loop nonlinear process systems with multiple inputs, various control architectures, and various control designs. This framework not only permits a fundamental understanding of the causes of the negative effects observed in control loops with valves for which the valve behavior cannot be neglected, but also enables a better understanding regarding how the tools previously developed in the literature for handling these dynamics work. This is critical for stiction compensation because a number of stiction compensation techniques are not model-based (and therefore the fundamental benefits and limitations of such stiction compensation strategies must be analyzed within a model-based framework) or are model-based but designed for specific linear process models, control architectures, and valve nonlinearity models. Furthermore, much of the stiction literature assumes that the system under study exhibits closed-loop oscillations due to stiction; notwithstanding some discussion regarding the causes of these oscillations in the literature, the conditions under which they do and do not occur for a general nonlinear chemical process under various control designs must be clarified. The developments of this work describe not only the causes of stiction-induced oscillations, but also the causes of improvements observed in the response of a closed-loop system with a sticky valve when a stiction compensation method is used. The developments are shown to permit the proposal of new stiction compensation schemes and to allow a number of perspectives on control design in light of valve behavior to be stated.

2. Preliminaries

2.1. Notation

The transpose of a vector x is denoted by x^T. The notation $u \in S(\Delta)$ signifies that the vector u is a member of the set of piecewise-continuous (from the right) functions with period Δ. The notation $t_k = k\Delta$, $k = 0, 1, 2, \ldots$, and the notation $\tilde{t}_j = j\Delta_e$, $j = 0, 1, 2, \ldots$, refer to elements of a time sequence separated by sampling time periods of lengths Δ and Δ_e, respectively. The notation $|\cdot|$ signifies the Euclidean norm of a vector.

2.2. Class of systems

We consider a nonlinear chemical process system with the following form:

$$\dot{x} = f(x, u_a, w) \tag{1}$$

where $x \in X \subseteq R^n$ is the process state vector (bounded in the set X), $u_a \in R^m$ is the vector of process inputs, $w \in R^l$ is a vector of bounded process disturbances (i.e., $w \in W := \{w \mid |w| \leq \theta\}$), and $f : R^n \times R^m \times R^l$ is a locally Lipschitz vector function of its arguments with $f(0, 0, 0) = 0$. Each component $u_{a,i}$, $i = 1, \ldots, m$, of the process input vector is an output of a valve that is adjusted utilizing a feedback controller for the nonlinear process that outputs a set-point $u_{m,i}$, $i = 1, \ldots, m$, for each valve output. Because the valve output flow rates are bounded by physical valve constraints, each input $u_{a,i}$ is bounded between a minimum ($u_{a,i,\min}$) and a maximum ($u_{a,i,\max}$) flow rate, with the resulting input constraint on u_a denoted by U (i.e., $u_a \in U$, where $U := \{u_a \in R^m \mid u_{a,i,\min} \leq u_{a,i} \leq u_{a,i,\max}, i = 1, \ldots, m\}$). Since the flow rates out of the valve are bounded, the set-points are bounded also (i.e., $u_m \in U_m$, where $U_m := \{u_m \in R^m \mid u_{m,i,\min} \leq u_{m,i} \leq u_{m,i,\max}, i = 1, \ldots, m\}$). The relationship between each $u_{m,i}$ and each $u_{a,i}$ depends on the valve behavior. We will consider valve behavior for which the $u_{a,i} - u_{m,i}$ relationship is either static or dynamic. In the case that the $u_{a,i} - u_{m,i}$ relationships are static, the following equation holds:

$$u_{a,i} = f_{static,\ i}(u_{m,i}) \tag{2}$$

where $f_{static,i}$ is a nonlinear vector function ($f_{static}(u_m) = [f_{static,1}(u_{m,1}) \cdots f_{static,m}(u_{m,m})]^T$). Alternatively, a dynamic model may characterize the $u_{a,i} - u_{m,i}$ relationship, where $u_{a,i}$ is related to both $u_{m,i}$ and the dynamic state vector $x_{dyn,i} \in R^{p_i}$, for which the components $x_{dyn,i,j}$, $j = 1, \ldots, p_i$, are states of the valve model. In this case, the following equations describe the dynamics of the ith valve:

$$\dot{x}_{\mathrm{dyn},i} = \hat{x}_{\mathrm{dyn},i}(x_{\mathrm{dyn},i}, u_{m,i}) \tag{3}$$

$$u_{a,i} = f_{\mathrm{dynamic},i}(x_{\mathrm{dyn},i}) \tag{4}$$

where $\hat{x}_{\mathrm{dyn},i}$ is a nonlinear vector function characterizing the dynamics of the internal states of the model for the ith valve, and $f_{dynamic,i}$ is a nonlinear vector function relating $u_{a,i}$ and the internal dynamic states of the valve. We define $x_{dyn} = [x_{dyn,1} \cdots x_{dyn,m}]^T$,

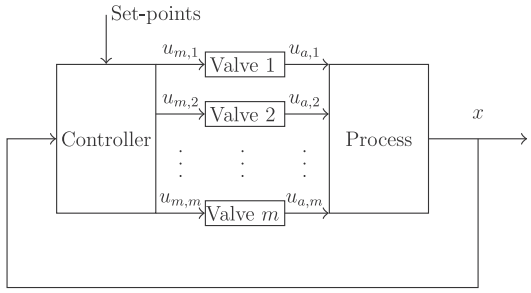

Fig. 1. Schematic showing the general control architecture under consideration in this work. A controller receives measurements of the process state x, as well as set-point information as appropriate, so that it can calculate m individual valve output flow rate set-points for m individual valves. The valves themselves have dynamics associated with developing a value of $u_{a,i}$, $i = 1, \ldots, m$, for a given $u_{m,i}$, $i = 1, \ldots, m$. The outputs of the valves act on the process to alter the state x.

$\hat{x}_{\text{dyn}}(x_{\text{dyn}}, u_m) = [\hat{x}_{\text{dyn},1}(x_{\text{dyn},1}, u_{m,1}) \cdots \hat{x}_{\text{dyn},m}(x_{\text{dyn},m}, u_{m,m})]^T$, and $f_{dynamic}(x_{dyn}) = [f_{dynamic,1}(x_{dyn,1}) \cdots f_{dynamic,m}(x_{dyn,m})]^T$.

We assume in this work that the value of each $u_{m,i}$ is determined utilizing a feedback controller (e.g., proportional-integral (PI) control or model predictive control (MPC), which will be placed in the notation of this section in the following two sections) that utilizes knowledge of at least one process state to compute control actions. This means that the value of each $u_{m,i}$ is affected by some subset of the state vector as follows:

$$u_{m,i} = f_{\text{controller},i}(x, \hat{\zeta}_i) \tag{5}$$

where $\hat{\zeta}_i \in R^{r_i}$, $i = 1, \ldots, m$, is a vector of internal states of the controller calculating $u_{m,i}$. These internal states may be dynamic as follows:

$$\dot{\hat{\zeta}}_i = f_{\text{internal},i}(x, x_{\text{dyn}}, \hat{\zeta}_i) \tag{6}$$

Defining $f_{\text{controller}}(x, \hat{\zeta}) = [f_{\text{controller},1}(x, \hat{\zeta}_1) \cdots f_{\text{controller},m}(x, \hat{\zeta}_m)]^T$, $\hat{\zeta} = [\hat{\zeta}_1 \cdots \hat{\zeta}_m]^T$, and $f_{\text{internal}}(x, x_{\text{dyn}}, \hat{\zeta}) = [f_{\text{internal},1}(x, x_{\text{dyn}}, \hat{\zeta}_1) \cdots f_{\text{internal},m}(x, x_{\text{dyn}}, \hat{\zeta}_m)]^T$, we can write the process-valve system as follows for the case of a static relationship between u_a and u_m (i.e., Eq. (2) holds):

$$\begin{bmatrix} \dot{x} \\ \dot{\hat{\zeta}} \end{bmatrix} = \begin{bmatrix} f(x(t), f_{\text{static}}(f_{\text{controller}}(x, \hat{\zeta})), w(t)) \\ f_{\text{internal}}(x, x_{\text{dyn}}, \hat{\zeta}) \end{bmatrix} \tag{7}$$

where $x_{dyn} = 0$ when Eq. (2) holds.

For the case of a dynamic relationship between u_a and u_m (i.e., Eqs. (3)–(4) hold), the following process-valve system results:

$$\begin{bmatrix} \dot{x} \\ \dot{x}_{\text{dyn}} \\ \dot{\hat{\zeta}} \end{bmatrix} = \begin{bmatrix} f(x(t), f_{\text{dynamic}}(x_{\text{dyn}}), w(t)) \\ \hat{x}_{\text{dyn}}(x_{\text{dyn}}, f_{\text{controller}}(x, \hat{\zeta})) \\ f_{\text{internal}}(x, x_{\text{dyn}}, \hat{\zeta}) \end{bmatrix} \tag{8}$$

With slight abuse of notation, the right-hand sides of both Eqs. (7) and (8) will be denoted by $f_q(q(t), u_m(t), w(t))$ (f_q signifies the right-hand side of Eq. (7) when Eq. (2) characterizes the $u_{a,i} - u_{m,i}$ relationship, and it signifies the right-hand side of Eq. (8) when Eqs. (3) and (4) characterize the $u_{a,i} - u_{m,i}$ relationship), where $q(t)$ represents the vector of process-valve states (i.e., $q = [x\ \hat{\zeta}]^T$ when Eq. (7) describes the process-valve dynamics, and $q = [x\ x_{\text{dyn}}\ \hat{\zeta}]^T$ when Eq. (8) describes the process-valve dynamics). We assume that f_q is a locally Lipschitz vector function of its arguments with $f_q(0, 0, 0) = 0$. The general principles of the control architectures described are illustrated in Fig. 1.

Remark 1. Disturbances could also be considered in other dynamic states of the process-valve model besides x, such as in x_{dyn}, and the analysis presented throughout this work would continue to hold.

2.3. Classical linear control with integral action

Linear control designs with an integral term are designed to drive a selected process output (here taken to be a process state, which is consistent with standard industrial practice in the chemical process industries) to its set-point. Thus, we assume that the process state vector or a subset of it comprises the vector $\hat{x} \in R^{\hat{n}}$, $\hat{n} \leq n$, of measured outputs being driven to the set-point vector $\hat{x}_{\text{sp}} \in R^{\hat{n}}$. When a PI controller is used, each component of $\hat{x}$ is regulated to its set-point by an individual linear controller that outputs a valve output flow rate set-point for an individual valve, and thus $\hat{n} = m$. The dynamics of the ith PI controller are represented by:

$$u_{m,i} = g_{A,i}(\hat{x}_i, \zeta_i) \tag{9}$$

$$\dot{\zeta}_i = A_{\text{con},i} \begin{bmatrix} \hat{x}_i \\ \zeta_i \end{bmatrix} + B_{\text{con},i} \hat{x}_{i,\text{sp}} \tag{10}$$

The form of these equations follows that in Eqs. (5) and (6), with $\hat{\zeta}_i = \zeta_i$, $f_{controller,i}$ given by $g_{A,i}$, and $f_{internal,i}$ given by the right-hand side of Eq. (10) . $A_{con,i}$ and $B_{con,i}$ are a matrix and scalar.

2.4. Model predictive control

Model predictive control (Qin and Badgwell, 2003; Ellis et al., 2014a) is an optimization-based control strategy based on the following optimization problem:

$$\min_{u_m(t) \in S(\Delta)} \int_{t_k}^{t_{k+N}} L_e(\tilde{x}(\tau), u_m(\tau))\, d\tau \tag{11a}$$

$$\text{s.t.} \quad \dot{\tilde{x}}(t) = f(\tilde{x}(t), u_m(t), 0) \tag{11b}$$

$$\tilde{x}(t_k) = x(t_k) \tag{11c}$$

$$\tilde{x}(t) \in X, \ \forall\ t \in [t_k, t_{k+N}) \tag{11d}$$

$$u_m(t) \in U_m, \ \forall\ t \in [t_k, t_{k+N}) \tag{11e}$$

$$g_{\text{MPC},1}(\tilde{x}(t), u_m(t)) = 0, \ \forall\ t \in [t_k, t_{k+N}) \tag{11f}$$

$$g_{\text{MPC},2}(\tilde{x}(t), u_m(t)) \leq 0, \ \forall\ t \in [t_k, t_{k+N}) \tag{11g}$$

The stage cost $L_e(x, u_m)$ is minimized subject to bounds on the states (Eq. (11d)), bounds on the inputs (Eq. (11e)), equality and inequality constraints (Eqs. (11f) and (11g)), and the restriction that the states must evolve according to the nominal ($w(t) \equiv 0$) dynamic model in Eq. (11b) when initialized from a measurement of the state (Eq. (11c)). $\tilde{x}(t)$ represents the process state according to the model of Eq. (11b) (i.e., in the absence of disturbances or plant/model mismatch) at time t; $x(t)$, on the other hand, represents the actual value of the state (which is affected by disturbances and thus is not necessarily the same as $\tilde{x}(t)$). By setting $\tilde{x}(t_k)$ to a measurement of the process state at t_k, the MPC becomes a feedback controller.

In Eq. (11b), $u_m(t)$ is used in place of $u_a(t)$ because the standard formulation of MPC in industry and the literature neglects valve behavior in general (i.e., it assumes that $u_a = u_m$; therefore, no reference is made to u_a in Eq. (11a)(11). MPC can, however, handle valve saturation through the constraint of Eq. (11e), assuming $u_a = u_m$. A vector of control actions u_m is computed for each of the N sampling periods of length Δ (N is the prediction horizon), and only the first of these vectors is applied to the process in a sample-and-hold fashion according to a receding horizon strategy. The notation $u_m^*(t|t_k)$, $t \in [t_k, t_{k+N})$, signifies the optimal value of u_m at time t for the optimization problem initiated at time t_k ($u_{m,i}^*(t|t_k)$ represents the ith component of this vector).

A form of MPC that is commonly used in the chemical process industries is tracking MPC, which drives $\hat{x}$ to $\hat{x}_{sp}$ (though it is not necessary in this case that $\hat{n} = m$) by utilizing a quadratic stage cost with its minimum at the set-point vector $\hat{x}_{sp}$ with corresponding steady-state input vector $u_{m,sp}$ as follows:

$$L_e(\tilde{x}(\tau), u_m(\tau)) = (\hat{x}_{sp} - \tilde{\hat{x}})^T Q_T (x_{sp} - \tilde{\hat{x}}) + (u_{m,sp} - u_m)^T R_T (u_{m,sp} - u_m) \quad (12)$$

where $Q_T > 0$ and $R_T > 0$ are tuning matrices, and $\tilde{\hat{x}}$ denotes the predicted value of the vector $\hat{x}$.

The value of each $u_{m,i}$ calculated by the MPC has the form of Eq. (5) with $\hat{\zeta}_i = 0$ (which leaves $u_{m,i}$ as a function of the process state), though the function $f_{controller,i}$ is not explicitly defined in this case but is defined implicitly by the optimization problem in Eq. (11a)(11).

Remark 2. We assume that full state feedback is available for all MPC designs presented in this work. When it is not, state estimation and output feedback MPC (e.g., Ellis et al., 2014) could be investigated to determine if they provide a suitable control design for a given system, but this will not be pursued here.

3. Process-valve model analysis: insights on impacts of valve behavior on closed-loop systems

Eqs. (7) and (8) comprise the unified framework that we develop in this work for analyzing the impacts of valve behavior and valve behavior compensation on control loop performance. They reveal that valve behavior changes the dynamics of a coupled closed- loop system. To see this, consider the system of Eq. (7), which represents a process-valve system subject to only a static valve nonlinearity under feedback control. The static nonlinearity impacts the dynamics of x (i.e., in the absence of the static valve nonlinearity ($u_a = u_m$), the dynamics of $\dot{x}$ would be described by $f(x(t), f_{\text{controller}}(x, \hat{\zeta}), w(t))$, which is different than the dynamics in Eq. (7)). In addition, both $\dot{x}$ and $\dot{\hat{\zeta}}$ are functions of x, so modifying f_{static} affects the dynamics of both x and $\hat{\zeta}$. Due to the fact that the system is nonlinear, the effect on the closed-loop response of changing f_{static} is difficult to determine without performing closed-loop simulations. This is particularly significant when there are multiple process inputs $u_{a,i}$ related to $u_{m,i}$ through different static nonlinear functions, especially assuming that the dynamics of the components of x are coupled. Then, each $u_{a,i}$ affects all components of x either directly or through coupling of those components in the vector function f, and the value of each $u_{a,i}$ is affected by all components of x due to the fact that the components of x are coupled and at least one of those components is used to calculate $u_{m,i}$ to define $u_{a,i}$ (Eq. (2)) due to the use of state feedback control (Eq. (5)). Using a similar analysis, it can be deduced that changing the control law (i.e., changing $f_{controller}$ and $f_{internal}$) also impacts the closed-loop response in a manner that is difficult to determine *a priori* (without simulations).

When the valve dynamics can be described by dynamic systems of equations as in Eq. (8), the dynamics of the valve, controller, and process are again coupled. In this case, however, there is an additional complexity in that the valve dynamics add additional states with nonlinear dynamics (or linear in the specific case of linear valve dynamics) that are not present in the case that $u_a = u_m$. Furthermore, because $u_{m,i}$ is a function of at least one of the components of x, it is affected by the other components of x as well, assuming coupling between these components. This causes $x_{dyn,i}$ and $u_{a,i}$ to also be related to x (Eqs. (3)–(4)), and the components of x are affected by the values of all $u_{a,i}$ in Eq. (1) and thus by all valve states $x_{dyn,i}$, $i = 1, \ldots, m$, from Eq. (4).

The above analysis shows that from a fundamental mathematical analysis of general equations for a process-valve system, the dynamics of all valves can be seen to be coupled with the dynamics of the other valves and also with the dynamics of the process and the controller due to state feedback (this is not limited to PI control or MPC). Because the controller dynamics affect the evolution of the states and thus the process outputs, different types of controllers would be expected to result in different responses of the process outputs. Furthermore, the control loop architecture will also affect the response because it will impact the equations that describe the controller dynamics. This analysis reveals that the negative effects of valve dynamics on control loop effectiveness are related to the controller, process, and valve dynamics, in addition to the control architecture. The next two sections make the notation of Eqs. (7) and (8) more concrete by showing how linear and sticky valve dynamics fit within that framework.

Remark 3. In this work, we consider a general case in which all states of the process-valve model are coupled. For cases when this does not hold, it may be possible to analyze the dynamics of the specific process to see if any simplifications result compared to the analysis in this work.

3.1. Linear valve dynamics

Linear valve dynamics can be denoted as follows:

$$\dot{x}_{u_{a,i}} = A_i x_{u_{a,i}} + B_i u_{m,i} \quad (13)$$

$$u_{a,i} = C_i x_{u_{a,i}} \quad (14)$$

where $x_{u_{a,i}} \in R^{p_i}$ is the vector of internal states of the linear valve dynamic model for the ith valve, and A_i, B_i, and C_i are a matrix and two vectors, respectively, of appropriate dimensions. Combining the process and valve layer models gives the following process-valve model for this case (omitting the dynamics of the controller):

$$\begin{bmatrix} \dot{x} \\ \dot{x}_{u_a} \end{bmatrix} = \begin{bmatrix} f(x(t), C_L x_{u_a}(t), w(t)) \\ A_L x_{u_a} + B_L u_m \end{bmatrix} \quad (15)$$

where A_L, B_L, and C_L are matrices and vectors of appropriate dimensions containing the elements of A_i, B_i, and C_i, $i = 1, \ldots, m$, in an appropriate order, and $x_{u_a} = [x_{u_{a,1}} \ \ldots \ x_{u_{a,m}}]^T$. Using the notation in Eqs. (3) and (4), $x_{\text{dyn}} = x_{u_a}$, and $\hat{x}_{\text{dyn},i}(x_{\text{dyn},i}, u_{m,i})$ and $f_{dynamic,i}(x_{dyn,i})$ equal the right-hand sides of Eqs. (13) and (14), respectively.

3.2. Sticky valve dynamics

For the case that all valves are sticky (i.e., affected by friction/stiction, which prevents the valve position from appreciably changing until the force applied to the valve moving parts becomes sufficiently large) and move in a straight line (rather than rotating), the valve position $x_{v,i}$ and the valve velocity $v_{v,i}$ for the $i-$th valve evolve in time according to the following force balance:

$$\dot{x}_{v,i} = v_{v,i} \quad (16)$$

$$\dot{v}_{v,i} = \frac{1}{m_{v,i}} (a_i^T F_{O,i} + c_i^T F_{A,i} - F_{\text{fric},i}) \quad (17)$$

where $m_{v,i}$ is the mass of the moving parts of the ith valve, $F_{O,i}$ is a vector of non-friction forces on the valve that are not related to the controller output or friction force and which have coefficient vector a_i, $F_{A,i}$ is a vector of non-friction forces on the valve that are adjusted based on the controller output and have coefficient vector c_i, and $F_{fric,i}$ is the friction force on the ith valve. The friction force is a static function of $x_{v,i}$, $v_{v,i}$, and $z_{f,i}$ (which is a dynamic internal state of the friction model), as follows:

$$F_{\text{fric},i} = \hat{F}_{\text{fric},i}(x_{v,i}, v_{v,i}, z_{f,i}) \quad (18)$$

$$\dot{z}_{f,i} = \hat{z}_{f,i}(x_{v,i}, v_{v,i}, z_{f,i}) \tag{19}$$

where $\hat{z}_{f,i}$ is a nonlinear vector function describing the dynamics of the internal states of the friction model.

Assuming that $F_{A,i}$ is a static function of $u_{m,i}$ as follows:

$$F_{A,i} = f_{SO,i}(u_{m,i}) \tag{20}$$

where $f_{SO,i}$ is a nonlinear vector function describing the relationship between $u_{m,i}$ and $F_{A,i}$, and that $F_{O,i}$ is also a function of the valve model states, the right-hand side of Eq. (17) can be denoted by $\hat{v}_{v,i}(u_{m,i}, x_{v,i}, v_{v,i}, z_{f,i})$. Finally, assuming that the relationship between $u_{a,i}$ and $x_{v,i}$ can be expressed through the following static nonlinear equation describing the valve characteristic:

$$u_{a,i} = f_{\text{flow},i}(x_{v,i}) \tag{21}$$

we obtain the following process-valve model (omitting the dynamics of the controller for the process):

$$\begin{bmatrix} \dot{x} \\ \dot{x}_v \\ \dot{v}_v \\ \dot{z}_f \end{bmatrix} = \begin{bmatrix} f(x(t), f_{\text{flow}}(x_v(t)), w(t)) \\ v_v \\ \hat{v}_v(u_m, x_v, v_v, z_f) \\ \hat{z}_f(x_v, v_v, z_f) \end{bmatrix} \tag{22}$$

where $x_v = [x_{v,1} \cdots x_{v,m}]^T$, $v_v = [v_{v,1} \cdots v_{v,m}]^T$, $z_f = [z_{f,1} \cdots z_{f,m}]^T$, $f_{\text{flow}}(x_v(t)) = [f_{\text{flow},1}(x_{v,1}) \cdots f_{\text{flow},m}(x_{v,m})]^T$, $\hat{v}_v(u_m, x_v, v_v, z_f) = [\hat{v}_{v,1}(u_{m,1}, x_{v,1}, v_{v,1}, z_{f,1}) \cdots \hat{v}_{v,m}(u_{m,m}, x_{v,m}, v_{v,m}, z_{f,m})]^T$, $\hat{z}_f(x_v, v_v, z_f) = [\hat{z}_{f,1}(x_{v,1}, v_{v,1}, z_{f,1}) \cdots \hat{z}_{f,m}(x_{v,m}, v_{v,m}, z_{f,m})]^T$. In the notation of Eq. (8), $x_{\text{dyn}} = [x_v\ v_v\ z_f]^T$, $f_{\text{dynamic}}(x_{\text{dyn}}) = f_{\text{flow}}(x_v(t))$, and $\hat{x}_{\text{dyn},i}(x_{\text{dyn},i}, u_{m,i})$ is given by the right-hand sides of Eqs. (16), (17) and (19).

4. Illustrating a closed-loop, systems perspective on the impacts of valve behavior on control loop performance

The closed-loop perspective on the impacts of valve behavior on control loop performance developed above provides a novel platform from which to fundamentally understand the conditions under which various negative effects attributed to valve behavior in control loops occur. In the next section, we show through an illustrative level control example that a prevalent phenomenon in the literature (stiction-induced oscillations) can only be explained through this closed-loop perspective. The simplicity of the example allows us to focus on the effects of the valve dynamics without the added complexity of a large-scale nonlinear process model; however, we subsequently elucidate the necessity of a closed- loop analysis for predicting the behavior of the measured outputs of a more complex process-valve system through a continuous stirred tank reactor (CSTR) example.

4.1. A closed-loop perspective on stiction-induced oscillations

In the level control problem (shown in Fig. 2) considered, the tank inlet flow rate u_a is the controlled variable. The dynamics of the tank level are:

$$\frac{\mathrm{dh}}{\mathrm{dt}} = \frac{1}{A}(u_a - c_1\sqrt{h}) \tag{23}$$

where $A = 0.25\ \mathrm{m}^2$ denotes the cross-sectional area of the tank, and $c_1 = 0.008333\ \mathrm{m}^{5/2}/\mathrm{s}$ is the outlet resistance coefficient. On an order of magnitude consistent with an example from Ogunnaike and Ray (1994) that uses these parameter values, the minimum tank height is 0 m, the maximum tank height is 0.5184 m, the minimum value of u_a is $u_{a,\min} = 0\ \mathrm{m}^3/\mathrm{s}$ (fully closed valve), and the maximum value of u_a is $u_{a,\max} = 0.006\ \mathrm{m}^3/\mathrm{s}$ (fully open valve).

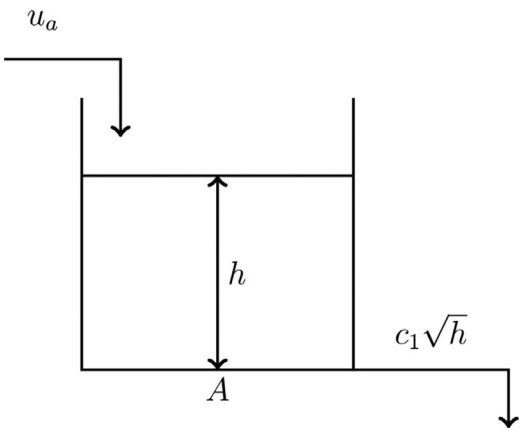

Fig. 2. Schematic depicting the tank considered in the level control example.

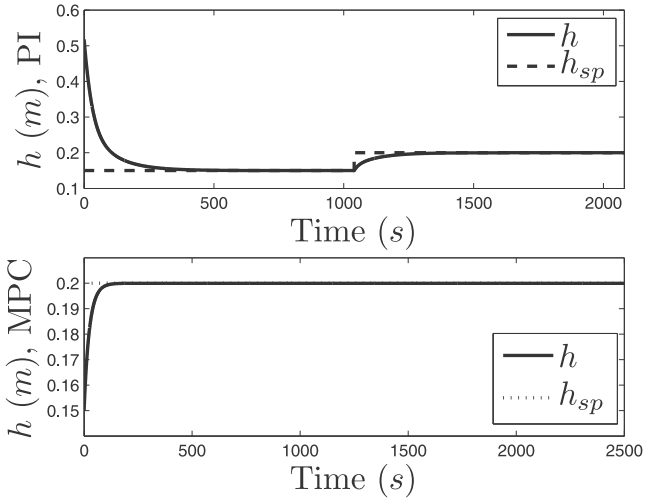

Fig. 3. Closed-loop trajectory of level h with reference to its set-point h_{sp} for the process of Eq. (23) under the PI controller of Eqs. (24) and (25) (top plot) and under the MPC of Eq. (26) (bottom plot) with no actuator dynamics.

4.1.1. Level control with negligible valve dynamics

When the valve dynamics are so fast that $u_a = u_m$ at all times is a reasonable approximation, a well-tuned PI controller and an MPC can be designed that effectively drive the level to its set-point. The PI controller for the tank level has the following form:

$$\dot{\zeta} = h_{\text{sp}} - h,\ \zeta(0) = 0 \tag{24}$$

$$u_m = u_{\text{as}} + K_c(h_{\text{sp}} - h) + K_c\zeta/\tau_I \tag{25}$$

where u_m is the controller output, ζ is the dynamic state of the PI controller, u_{as} is the steady-state value of u_a before the set-point change, and h_{sp} is the level set-point. A tuning $K_c = 0.006$ and $\tau_I = 43.2$ was selected that prevents u_m from dipping below $u_{a,\min}$ or shooting above $u_{a,\max}$ for the set-points simulated. The response of the level of the tank of Eq. (23) under the PI controller of Eqs. (24)–(25) when $u_a = u_m$ is shown in the top plot of Fig. 3, plotted every 100 integration steps, for the tank level initiated from its maximum ($u_a = 0.006\ \mathrm{m}^3/\mathrm{s}$, $h = 0.5184$ m), decreased to 0.15 m, and then increased to 0.20 m (the set-point change from 0.15 m to 0.20 m will be the focus in the remainder of this section to avoid the effects of possible initial transients during the first set-point change). Each set-point was held for 1040 s. The dynamic system was integrated with the explicit Euler numerical integration method and an integration step size of 10^{-3} s. At the set-point changes, the value of ζ was re-set to 0 and the value of u_{as} was set to the last applied value of u_m.

Focusing on the second set-point change from the example above, we also design a well- tuned tracking MPC to drive the level from 0.15 m to 0.20 m when $u_a = u_m$ as follows:

$$\min_{u_m(t)\in S(\Delta)} \int_{t_k}^{t_{k+N}} Q_T(h_{sp} - \tilde{h})^2 + R_T(u_{a,sp} - u_m)^2 \, d\tau \tag{26a}$$

$$\text{s.t.} \quad \dot{\tilde{h}} = \frac{1}{A}(u_m - c_1\sqrt{\tilde{h}}) \tag{26b}$$

$$\tilde{h}(t_k) = h(t_k) \tag{26c}$$

$$0 \le u_m(t) \le 0.006, \ \forall\, t \in [t_k, t_{k+N}) \tag{26d}$$

where $Q_T = 0.00001$ and $R_T = 1$. Using this MPC to control the process of Eq. (23) with an integration step size of 10^{-3} s within the MPC, an integration step size of 10^{-5} s to simulate the level, a prediction horizon of $N = 50$, a sampling period of length $\Delta = 1$ s, a final time of the simulation of 2500 s, and a set-point $h_{sp} = 0.20$ m with its corresponding steady-state flow rate $u_{a,sp} = 0.00373$ m^3/s, the state profile in the bottom plot of Fig. 3 is obtained (the results are plotted every 10 000 integration steps). The nonlinear interior point optimization solver Ipopt (Wächter and Biegler, 2006) was used for the simulations with a tolerance of 10^{-8} on a 2.40 GHz Intel Core 2 Quad CPU Q6600 on a 64-bit Windows 7 Professional operating system with 4.00 GB of RAM.

Remark 4. The closed-loop responses of the level under the PI and MPC designs are not meant to be compared with one another. The purpose of Fig. 3 is to show that under both PI control and under MPC, when $u_a = u_m$, the tunings that are used for the level control example result in very good set-point tracking of the level. The results for the PI controller and MPC in Fig. 3 will be compared with the results utilizing the same tunings when $u_a \neq u_m$ for each controller in the following section.

4.1.2. Level control with a sticky valve

When only the valve dynamics change compared to the case in the prior section (i.e., the valve becomes sticky), sustained oscillations are set up in the originally well-tuned control loops. For this sticky valve case, u_a in Eq. (23) is the flow rate out of a pressure-to-close spring-diaphragm sliding-stem globe valve actuated by a pressure P. If the valve is initiated from its fully open position, no pressure is initially applied and the valve stem is at its equilibrium position $x_v = 0$ m. Its fully closed position corresponds to $x_v = x_{v,\max} = 0.1016$ m. The differential equations for the valve dynamics are (Garcia, 2008):

$$\frac{dx_v}{dt} = v_v \tag{27}$$

$$\frac{dv_v}{dt} = \frac{1}{m_v}[A_v P - k_s x_v - F_f] \tag{28}$$

where A_v and k_s are the diaphragm area and spring constant, respectively, and the friction force F_f is determined from the LuGre friction model (Canudas de Wit et al., 1995):

$$F_f = \sigma_0 z_f + \sigma_1 \frac{dz_f}{dt} + \sigma_2 v_v \tag{29}$$

$$\frac{dz_f}{dt} = v_v - \frac{|v_v|\sigma_0}{F_C + (F_S - F_C)e^{-(v_v/v_s)^2}} z_f \tag{30}$$

The parameters of the valve dynamic model in Eqs. (27)–(30) are those for the "nominal valve" in Garcia (2008) and are displayed in Table 1. In addition, we assume that the valve has a linear installed characteristic (Coughanowr and LeBlanc, 2009):

$$u_a = \left(\frac{x_{v,\max} - x_v}{x_{v,\max}}\right) u_{a,\max} \tag{31}$$

Table 1
Valve model parameters (Garcia, 2008).

Parameter	Value
m_v	1.361 kg
A_v	0.06452 m^2
k_s	52538 kg/s^2
v_s	0.000254 m/s
σ_0	10^8 kg/s^2
σ_1	9000 kg/s
σ_2	612.9 kg/s
F_C	1423 kg m/s^2
F_S	1707.7 kg m/s^2

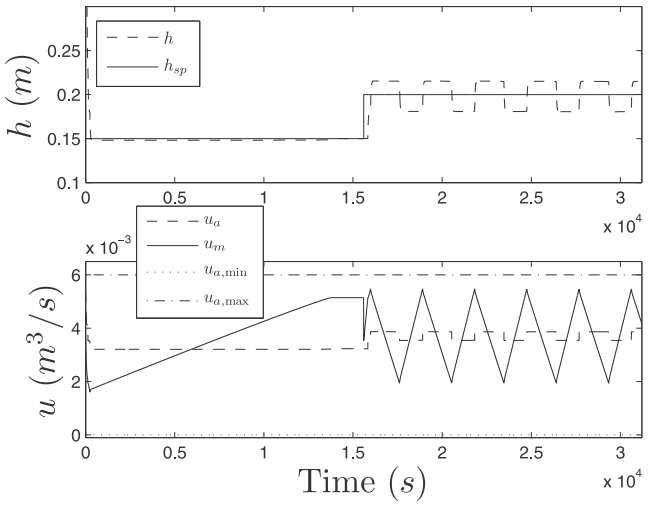

Fig. 4. Closed-loop trajectories of h, u_a, and u_m for the process of Eq. (23) under the PI controller of Eqs. (24) and (25) with the valve dynamics in Eqs. (27)–(32). This data is plotted every 100 000 integration steps. The values of $u_{a,\min}$ and $u_{a,\max}$ are plotted to indicate the range of allowable flow rates through the valve.

The pressure to be applied to the valve for a given set-point u_m is determined from the following $u_m - P$ relationship that was developed for a low-stiction valve in Durand and Christofides (2016) (though the tunings developed in the no-stiction case perform well for the low-stiction valve):

$$P = \frac{(u_m/u_{a,\max}) - 0.70391/0.7042}{-\frac{0.05864}{6894.76*0.7042}} \tag{32}$$

This relationship has the form of Eq. (20), where P is $F_{A,i}$ and the right-hand side of Eq. (32) is $f_{SO,i}(u_m)$.

Fig. 4 shows h, u_m, and u_a when the valve with the dynamics in Eqs. (27)–(32) is used to adjust the flow rate to the process of Eq. (23) under the PI controller of Eqs. (24) and (25). The valve was initiated from its fully open position (i.e., $h = 0.5184$ m, $u_a = 0.006$ m^3/s, $\zeta = 0$ m s, $x_v = 0$ m, $v_v = 0$ m/s, $z_f = 0$ m), and the set-point was changed to 0.15 m for 15 600 s, then to 0.20 m for 15 600 s. Because the second set-point change is the focus in this work, we will refer to the process-valve state at $t = 15\,600$ s from this simulation as q_l (the initial process-valve state for the level set-point change from 0.15 m to 0.20 m). The value of ζ was re-set to zero when the level set-point was changed, and the value of u_{as} in Eq. (25) was re-set to the last applied value of u_a when the set-point was changed. The trajectories were obtained using the explicit Euler numerical integration method with an integration step size of 10^{-5} s. In the simulations of the valve, several physical considerations are taken into account: if $u_m > u_{a,\max}$ or $u_m < u_{a,\min}$, u_m is saturated at $u_{a,\max}$ or $u_{a,\min}$ respectively; if $P < 0$, P is set to 0; if $u_a > u_{a,\max}$ or $u_a < u_{a,\min}$, u_a is saturated at $u_{a,\max}$ or $u_{a,\min}$ respectively.

Choudhury et al. (2005) notes that the impetus for the oscillations is related to the friction force dynamics and PI controller dynamics. Specifically, the friction force dynamics are such that F_f decreases rapidly when the valve begins to move (a contributor to this is that the parameter F_S, which represents the static friction coefficient, is larger than F_C, which represents the Coulomb friction coefficient) which creates a large and rapid change in $\frac{dv_v}{dt}$, leading the valve position to overshoot its value associated with h_{sp}. In the following, we discuss this in detail in terms of coupling of the process states. The fact that the dynamics of the various states play a role in the response observed will be exemplified by analyzing numerical data from the simulation performed (the exact numbers reported are related to the integration step size utilized, but the general effects would be expected to extend qualitatively to other integration step sizes) between the times $\bar{t}_1 = 17\,608.72441$ s and $\bar{t}_2 = 17\,608.72597$ s in Fig. 4.

Between $\bar{t}_1$ and $\bar{t}_2$, P only increases from 55 942.138 to 55 942.181 Pa (the force due to the pressure changes only by 0.0027 N) due to the dynamics of the PI controller within the coupled nonlinear process, and x_v changes only slightly (from 0.036236 m to 0.036295 m) as well. However, F_f changes from 1700.022 N at $\bar{t}_1$ to 1501.874 N at $\bar{t}_2$ (i.e., it decreases by close to 200 N), causing the right-hand side of Eq. (28) to increase from 4.1304 N/kg at $\bar{t}_1$ to 147.4380 N/kg at $\bar{t}_2$ because though the first two terms related to P and x_v do not change much, the term for the friction force decreases significantly. When the right-hand side of Eq. (28) increases, the valve velocity increases, which can cause the valve to move. This shows that though the drop in the friction force played an important role in adjusting the valve velocity, the dynamics of the PI controller and the stem position also played a role by not allowing P and x_v to adjust rapidly when F_f decreased. Furthermore, the dynamics of the level play a role in adjusting P as well since the PI controller depends on h in relation to its set-point. Additionally, the magnitude of the integral term of the PI control law is significantly larger than magnitude of the proportional term when the level changes and overshoots its set-point, which may also impact the length of time that the valve is stuck.

The fact that the negative effect of stiction in a control loop is a closed-loop property of a full process-valve system is further emphasized by utilizing the MPC of Eq. (26) (i.e., an MPC that accounts only for the level dynamics and not the actuator dynamics) for the set-point change from 0.15 m to 0.20 m for the process-valve system of Eqs. (23) and (27)–(32), initiated from q_I. The process was integrated with an integration step size of 10^{-6} s using the explicit Euler numerical integration method. The resulting trajectories of the level under the MPC are shown in Fig. 5, plotted every 1000 integration steps (the values of h, u_a, and u_m for this case are denoted in the legend by U, signifying that stiction is uncompensated in these results because the MPC does not account for the actuator dynamics). No oscillations are observed for this level set-point change as in Fig. 4, demonstrating that the stiction-induced oscillations observed under the PI controller depend on the controller utilized. Instead of oscillations, a persistent offset from the set-point occurs under the MPC. The reason for this is that because the MPC is unaware of the actuator dynamics, it calculates values of u_m that correspond to pressures (through Eq. (32)) that do not allow the valve to move according to the force balance (i.e., the MPC expects that the control actions that it calculates will drive the level toward the set-point because it is anticipating that there is no friction in the valve, but due to friction the valve cannot move with the pressure applied to it). The MPC continues to compute approximately the same control action for the first sampling period of the prediction horizon at each sampling time (which is reasonable considering that the state measurement that it receives is approximately the same each time since the valve is stuck and thus the flow rate out of the valve is

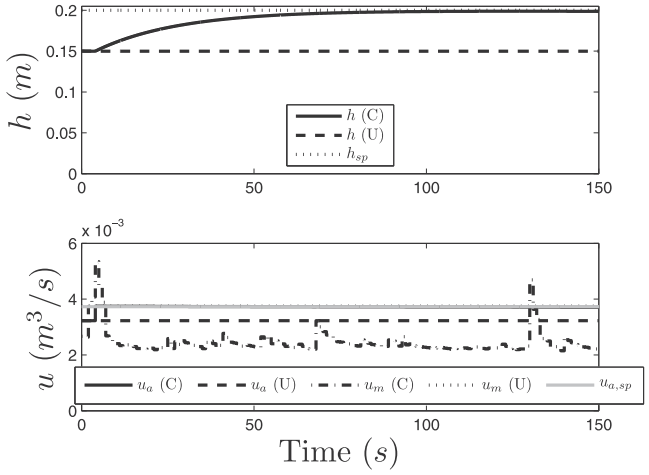

Fig. 5. Plot of trajectories of h, u_a, u_m, and their set-points for the MPC of Eq. (26) (U, signifying "uncompensated") and the MPC of Eq. (41) (C, signifying "compensated") applied to the nonlinear process of Eqs. (23) and (27)–(32) for a level set-point change from 0.15 m to 0.20 m.

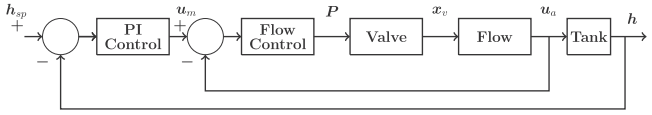

Fig. 6. Schematic depicting the control architecture for the level control example with flow control. In the inner loop, the flow controller computes the pressure P from the pneumatic actuation, which then alters the position x_v of the sticky valve according to the valve dynamics (labeled as "Valve" in the figure). The valve position x_v is related to the flow u_a through the valve according to the linear valve characteristic of Eq. (31) (labeled as "Flow" in the figure).

not appreciably changing to adjust the level). This control action continues to be unable to affect the level appreciably, resulting in persistent off-set of the level from h_{sp} because the MPC has no mechanism for detecting that the set-points it has calculated are failing to make an impact on the system.

Returning again to the control loop under PI control, we now show that a change in the control loop architecture (in this case, adding flow control to the valve of Eqs. (27)–(31)) alters the response of the process outputs. The control loop architecture in this case is depicted in Fig. 6 , where the flow rate set-point u_m is computed by the PI controller of Eqs. (24) and (25) for the tank level, and becomes the set-point for a minor PI control loop used to regulate u_a to u_m. This minor loop calculates the pressure P to be applied to the valve stem based on the error $u_m - u_a$ as follows:

$$P = P_s + K_{c,p}\frac{u_m - u_a}{u_{a,\max}} + \frac{K_{c,p}}{\tau_{I,p}}\zeta_P \tag{33}$$

$$\dot{\zeta}_P = \frac{u_m - u_a}{u_{a,\max}},\ \zeta_P(0) = 0 \tag{34}$$

where P_s is the steady-state value of the pressure, and $K_{c,p} = -82\,737.09$, $\tau_{I,p} = 0.01$, and ζ_P are the proportional gain, integral time, and internal state, respectively, of the minor loop controller. The tuning (from Durand and Christofides (2016)) performed successfully when u_m was constant for some time.

The valve was initially operated without flow control (i.e., Eq. (32) was used to relate u_m and P) for 15 600 s for a level set-point change from 0.5184 m to 0.15 m to reach q_I. Subsequently, it was operated under the flow controller of Eqs. (33) and (34) for 15 600 s for the level set-point change from 0.15 m to 0.20 m. Fig. 7 shows the responses of h, u_m, and u_a for the set-point change from 0.15 m to 0.20 m (the time axis is short to display the fast response of the valve under flow control). These results were obtained using an integration step size of 10^{-5} s, with the data plotted every 100 000 integration steps. The integral term ζ_P

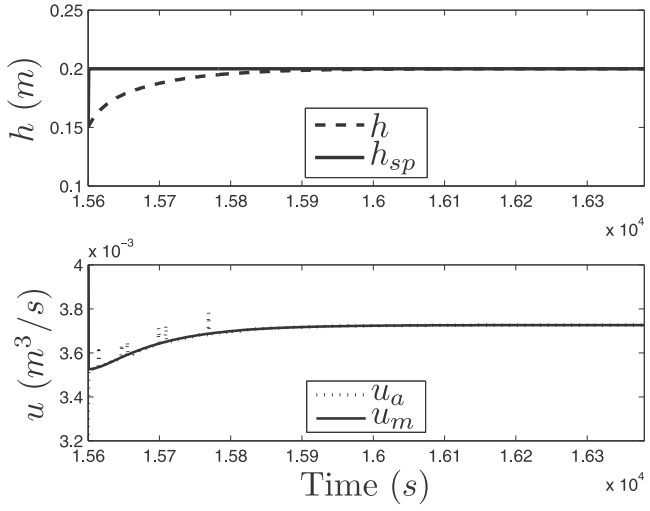

Fig. 7. Closed-loop trajectories of h, u_a, and u_m for the process of Eq. (23) under the PI controller of Eqs. (24) and (25) with the valve in Eqs. (27)–(31) and the PI controller of Eqs. (33) and (34) used to control the valve flow rate to its set-point value for the set-point change from 0.15 m to 0.20 m.

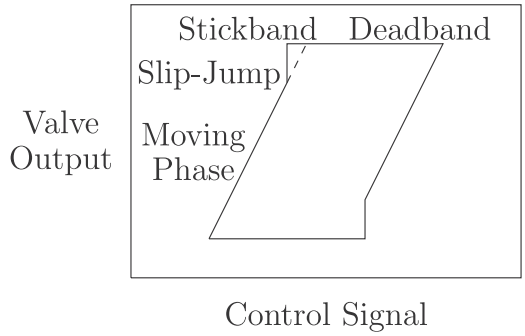

Fig. 8. Standard controller input-valve output relationship reported for a sticky valve. The control signal to the valve changes but the valve output does not change appreciably in the regions of deadband and stickband. The valve output changes quickly in the region of slip-jump, and the valve output and control signal are linearly related in the moving phase region of the response.

of the controller for the valve was re-set to zero when the level set-point was changed, and at that point the value of P_s was also re-set to the last applied pressure.

The sustained oscillations apparent in Fig. 4 do not appear in Fig. 7, though the same process, sticky valve, and outer loop PI controller are used as in Fig. 4. This is particularly notable given that the friction dynamics and the right-hand side of Eq. (17) have not changed (i.e., the change is essentially in the manner in which P is calculated; the coupling among the states of the process-valve model causes the change in the system dynamics resulting from the addition of the dynamic PI flow controller to alter the level response compared to the case without flow control). Instead of oscillations, when flow control is used, u_a tracks u_m well after it initially overshoots u_m in the time period immediately after the set-point change. During these initial overshoots, the pressure applied to the valve changed rapidly according to Eqs. (33) and (34), and the forces on the valve resulted in the initial significant overshoots of u_a around the changing u_m set-point. However, despite these initial overshoots of u_a, the flow controller is successful at stabilizing the level at its set-point (it causes the forces on the valve to balance in such a manner that u_a is able to track u_m and thus to drive the level to its set-point). The change of the control loop architecture changed the number of coupled dynamic states in the system of nonlinear differential equations describing the process-valve system (i.e., whereas the state vector of the process-valve system without flow control included h, ζ, x_v, v_v, and z_f, it also includes ζ_P when flow control is used). Returning to the notation of Eq. (8), this means that x_{dyn} incorporates an extra state and its dynamics when flow control is used, which overall changes the response of the measured output (h) of the process-valve system compared to the case without flow control.

Remark 5. The analysis performed demonstrates that the standard valve output-controller input response for a sticky valve exhibited in Fig. 8 (and displayed in multiple sources in the literature such as Choudhury et al. (2005) and Brásio et al. (2014)) can be understood as the response of the valve output when the force applied to the valve is ramped up and down by a controller (i.e., the closed-loop analysis above indicates that the "controller output" on the standard plots is linked to the force applied to the valve). Furthermore, Fig. 8 reflects the transient behavior of the valve after it begins moving (i.e., it shows the slip-jump). This is in contrast to Fig. 6 in Durand and Christofides (2016), which is a plot of the relationship between u_a and the pressure applied to two valves, one with low and one with more significant stiction, as the pressure is ramped up and down, but plotting only the final values of u_a and P at the end of each time period for which P is held constant (rather than throughout the transient as u_a adjusts to a P change). Furthermore, in Fig. 8 in Durand and Christofides (2016) , the pressure is ramped up and down independently of a controller or process (i.e., the valve is analyzed alone); however, in plots like those in Fig. 8 of the present work, which explicitly assume the use of a controller and thereby imply that the plot comes from measurements of a process-valve system, the coupling of the controller, process, and valve dynamics for that process-valve system may cause a plot of u_a versus the force applied to the valve to be different when the same valve is operated under a different controller or for a different process. For example, for the level control problem without flow control, the plot of u_a versus P does not have a significant moving phase because soon after the valve slips, the controller begins to drive the valve in the opposite direction. Because the plot can also be understood as the valve position x_v (rather than u_a) versus the controller signal as in Ivan and Lakshminarayanan (2009), a linear valve characteristic is assumed when the same plot is obtained for u_a versus the controller signal.

4.2. A closed-loop perspective for a CSTR example

We now demonstrate the necessity of a closed-loop perspective for analyzing a process- valve dynamic system when the complexity of the process model increases (i.e., it has more states and inputs than the level control problem). For illustration purposes, we examine the production of ethylene oxide from ethylene in a CSTR with a heating/cooling jacket. Using the reaction rate equations for this process from Alfani and Carberry (1970), the following nonlinear process equations are obtained (in dimensionless form) from mass and energy balances on the reactor (Özgülşen et al., 1992):

$$\dot{x}_1 = u_{a,1}(1 - x_1 x_4) \tag{35a}$$

$$\dot{x}_2 = u_{a,1}(u_{a,2} - x_2 x_4) - A_1 \exp(\gamma_1/x_4)(x_2 x_4)^{0.5} - A_2 \exp(\gamma_2/x_4)(x_2 x_4)^{0.25} \tag{35b}$$

$$\dot{x}_3 = -u_{a,1} x_3 x_4 + A_1 \exp(\gamma_1/x_4)(x_2 x_4)^{0.5} - A_3 \exp(\gamma_3/x_4)(x_3 x_4)^{0.5} \tag{35c}$$

$$\dot{x}_4 = \frac{u_{a,1}}{x_1}(1 - x_4) + \frac{B_1}{x_1}\exp(\gamma_1/x_4)(x_2x_4)^{0.5} + \frac{B_2}{x_1}\exp(\gamma_2/x_4)(x_2x_4)^{0.25} + \frac{B_3}{x_1}\exp(\gamma_3/x_4)(x_3x_4)^{0.5} - \frac{B_4}{x_1}(x_4 - u_{a,3}) \quad (35d)$$

where x_1, x_2, x_3, and x_4 are dimensionless quantities corresponding to the gas density, ethylene concentration, ethylene oxide concentration, and temperature in the reactor, and the process inputs $u_{a,1}$, $u_{a,2}$, and $u_{a,3}$ are dimensionless quantities corresponding to the feed volumetric flow rate, feed ethylene concentration, and coolant temperature, which are assumed to be adjusted by individual valves either directly (e.g., $u_{a,1}$) or indirectly (e.g., $u_{a,2}$ may be adjusted by opening or closing valves that allow a more concentrated ethylene stream to mix with a solvent stream, and $u_{a,3}$ may be adjusted by heating or cooling the coolant using a higher or lower flow rate of another fluid past the coolant in a heat exchanger). Due to the coupling between the states in Eq. (35), and the highly nonlinear dynamic equations, it is difficult to predict the evolution of x_1, x_2, x_3, and x_4, regardless of the type of controller used to calculate $u_{m,1}$, $u_{m,2}$, and $u_{m,3}$, and even if $u_{a,1} = u_{m,1}$, $u_{a,2} = u_{m,2}$, and $u_{a,3} = u_{m,3}$. Therefore, if the valves also have dynamics, linear or nonlinear, static or dynamic, or potentially different dynamics for each valve, and different controllers or control loop architectures for each valve, the number of coupled states in this system of nonlinear differential equations increases and performing simulations will be the best way to understand how each process output will respond.

5. Implications of a unified process-valve system framework for valve behavior compensation and modeling

The closed-loop perspective regarding valve behavior clarifies how and when valve behavior compensation strategies in the literature work (to demonstrate this, we will review several stiction compensation methods) and enables valve behavior compensation designs to be proposed that target the coupling of the states that leads to negative effects (which we will demonstrate by describing how two of our valve behavior compensation strategies, an integral term modification method for processes with sticky valves under PI control and an MPC-based general valve behavior compensation technique, can be understood in a closed-loop context). Because a full process-valve system model is required to predict the response of the process and valve outputs under various valve behavior compensation methods and potentially is needed by those compensation schemes to allow them to compute compensating signals to adjust the closed-loop response, we also examine the practical question of how an empirical model that captures the dominant process-valve dynamics may be obtained when a first-principles model is unavailable or undesirable to use. Finally, we will exemplify the discussion through several process examples.

5.1. A closed-loop dynamic analysis of the stiction compensation literature

We analyze three categories of methods from the stiction compensation literature (more thorough reviews of stiction compensation methods have been provided elsewhere; see, for example, Brásio et al. (2014); Cuadros et al. (2012); Mohammad and Huang (2012)). The novelty of the analysis of this section lies in presenting several of these methods within the closed-loop systems framework described above to provide a fundamental understanding of how they ameliorate the negative effects observed in control loops with sticky valves, and their benefits and limitations.

5.1.1. Stiction compensation methods: controller tuning adjustments

Re-tuning of controllers has been advocated as a method for reducing closed-loop oscillations developed in a control loop containing a sticky valve under classical proportional-integral-derivative (PID)- type control (e.g., Mohammad and Huang (2012)). The re-tuning may result in an improved closed-loop response because it changes the dynamics of the PID-type controller, which alters the response of the process outputs due to the coupling of the controller, process, and valve dynamics. Thornhill and Horch (2007) highlights the difficulty of determining an appropriate tuning for obtaining a desired response, which is consistent with the difficulty of predicting, *a priori*, the response of a nonlinear dynamic system.

5.1.2. Stiction compensation methods: augmented controller signal

The knocker (Hägglund, 2002; Srinivasan and Rengaswamy, 2005) and constant reinforcement (Ivan and Lakshminarayanan, 2009) adjust the control signal received by the valve by adding either a constant or time-varying signal to the input calculated by the controller. This changes the manner in which the force applied to the valve is calculated. For example, consider the knocker applied to the level control example without flow control. The PI controller has its own dynamics that, in the absence of the knocker, dictate the pressure applied to the valve. However, with the knocker, there are times when the pressure applied to the valve is increased by an amount determined by the knocker parameters above the amount output by the PI controller, but then after a certain time period, the knocker takes away that extra amount of pressure. This allows the PI controller to retain its dynamics but permits the pressure to be adjusted using a source other than the PI controller as well, which changes the balance of forces on the valve/the process-valve dynamics and can result in a different closed-loop response than would be obtained without the knocker. Changes to the knocker parameters change the closed-loop system dynamics and as a result the closed-loop response as observed in Srinivasan and Rengaswamy (2005).

Constant reinforcement similarly augments the output of the PI controller, adding a constant positive signal when the PI controller output is increasing and a constant negative signal when the PI controller output is decreasing, which again changes the right-hand side of the equation for the valve velocity compared to not adding such a signal. One aspect of the effect of this on the level control problem might be, for example, that the integral term of the PI controller may not need to become as large for the pressure from the pneumatic actuation to overcome the static friction force and cause the valve to move. A method proposed by Cuadros et al. (2012) for turning off the PID-type controller and the knocker is an extension of the knocker method, but as noted by Wang (2013) and clarified through the closed-loop analysis in this work, the knocker changes the force balance/closed-loop dynamics but that does not guarantee that there will be no offset between the process output and its set-point if the PID controller is removed so thus removing the controller and compensating pulses may not be appropriate.

5.1.3. Stiction compensation methods: two moves method

The two moves method (Srinivasan and Rengaswamy, 2008) specifies compensating signals to apply to the signal coming from a linear controller that will drive the stem position to its set-point. This method is model-based, which means that it has accounted for the coupling of the process- valve dynamics, and a number of assumptions are required to guarantee that the method can drive

the valve position to its set-point, including that a particular data-driven stiction model is an exact representation of the stiction dynamics and that there are no disturbances or plant-model mismatch. A method similar in concept to the two moves method (it determines how to change the set-points for a closed-loop system in a manner that brings the valve position to a desired value) is developed in Wang (2013) and is inspired by a process-valve model for processes that can be described with a linear model and are under linear control.

5.2. Motivating valve behavior compensation design with closed-loop dynamic analyses

In this section, we seek to encourage further research on valve behavior compensation based on the closed-loop perspective on valve behavior developed in this work. To do this, we describe how two of our recent stiction compensation methods can be motivated by this framework.

5.2.1. Stiction compensation methods: integral term modification

The controller tuning adjustment methods discussed above require a controller's tuning to be changed even if the tuning being utilized is known to work well for the valve when it is not sticky and thus would be the preferred tuning after valve maintenance is performed. Furthermore, the nonlinearity of the stiction phenomenon, the coupling between the process states, and the complexity of the manner in which the forces on the valve balance and come out of balance makes it difficult to discern *a priori* what the best tuning to use when the valve is sticky should be. Therefore, it is reasonable to consider whether there is another method of adjusting a PI controller's dynamics instead of disrupting the desired tuning in an *ad hoc* fashion.

One such method is to add a term to the integral action of the linear controller that can easily be removed or adjusted for any set-point change to attempt to alleviate stiction-induced oscillations. Given that a characteristic of the stiction-induced oscillations is that the valve output u_a does not track its set-point u_m, this added term can be based on the scaled difference between u_a and u_m. Specifically, for a PI controller for which ζ signifies the integral of the error between the process output set-point (assuming a single output denoted by $\hat{x}_{sp}$) and the process output ($\hat{x}$, assumed to be a component of the process state vector), the following control law defines the control action with an integral term modification:

$$u_m = u_{as} + K_c(\hat{x}_{sp} - \hat{x}) + K_c\zeta/\tau_I \tag{36}$$

$$\dot{\zeta} = \begin{cases} (\hat{x}_{sp} - \hat{x}) + L(u_a - u_m), & t < t_{AW} \\ (\hat{x}_{sp} - \hat{x}) + \mathrm{Le}^{(-\beta(t-t_{AW}))}(u_a - u_m), & t \geq t_{AW} \end{cases}$$
$$\zeta(0) = 0 \tag{37}$$

where L, β, and t_{AW} are tuning parameters that can be adjusted by a control engineer to attempt to mitigate stiction-induced oscillations. When $L = 0$, Eq. (37) reduces to the standard integral term in a PI control law, and thus has no effect. The parameters are best determined using closed-loop simulations and/or on-line adjustments of L, β, and t_{AW}; however, the general goals of adjusting the parameters provide a potential methodology for looking for an appropriate tuning. In particular, the goal of this method is to determine a tuning that can decrease $\dot{\zeta}$ in such a way that the forces on the valve equilibrate at a value that causes the controlled process output to meet its set-point. By choosing a value of L that causes the term $L(u_a - u_m)$ in Eq. (37) to have a sign opposite to that of the term $(\hat{x}_{sp} - \hat{x})$, it is possible to cause $\dot{\zeta}$ to decrease even before $\hat{x} = \hat{x}_{sp}$ (this would not be possible with the standard PI control law, for which the integral term can only begin to decrease after the set-point is exceeded). Therefore, a possible strategy for tuning the term containing L in Eq. (37) is by first setting β and t_{AW} to zero, and then searching for a value of L that is able to cause $\dot{\zeta}$ to equal zero and drive $\frac{dv_v}{dt}$ to zero by providing a constant force from the valve actuation. This may occur, however, before $\hat{x}_{sp}$ is reached, resulting in offset. Therefore, the value of t_{AW} may be set to a time at which the forces on the valve appear to no longer be changing and that allows $\hat{x}$ to begin to approach its set-point as soon as possible after this has occurred. Then, various values of β may be tried to attempt to decrease the term containing L in ζ, which can cause this integral term to change and thus changes the force applied to the valve as a result of the control action u_m received by the valve. If a value of β can be found that changes the force applied to the valve in a manner that causes the forces to once again become constant, but this time at a value of the valve position that causes $\hat{x}_{sp}$ to be reached, then this control strategy is successful for the set-point change examined. However, some values of β may even cause stiction-induced oscillations to be set up once again even if the value of L examined was able to attenuate them before the time t_{AW}; this shows that the tuning problem is complex and that an appropriate tuning cannot be decided *a priori*. In addition, due to the nonlinearities in the valve and process dynamics, and the potential for interactions between states and inputs, there is no guarantee that any appropriate tuning will be found for a given set-point change, or that the same tuning will work for a variety of set-point changes or disturbances; however, closed-loop simulations or on-line adjustment can be attempted to see if there are values of L, β, and t_{AW} that are generally appropriate for a given process. Notably, when the integral term modification method is utilized in the case of bounded, time-varying process disturbances, which is the case considered in this work according to the class of process systems in Section 2.2, the notion of driving the output to the set-point does not exist (instead, it would be hoped that the controller could drive the state to an acceptably small neighborhood of the set-point). Various tunings could be evaluated for the integral term modification in this case to determine if they are able to do so.

5.2.2. Valve behavior compensation methods: MPC for valve behavior compensation

The closed-loop perspective on valve behavior indicates that a compensation method that accounts for the process-valve dynamics when computing control actions would be able to systematically address the root cause of the negative effects observed in control loops with valves that have behavior that cannot be neglected. An MPC design that uses the process-valve model to make state predictions is able to do this. An MPC design with a general objective function that incorporates a process-valve model including sticky valve dynamics was developed in Durand and Christofides (2016). It can account for multiple sticky valves, even with differing levels of stickiness, and has the ability to incorporate constraints that guarantee feasibility and closed-loop stability of a nonlinear process operated under the controller. In general, any process-valve model can be used within this MPC framework, so it could be considered for valve behavior compensation in general (i.e., it is not specific to stiction). This allows the MPC to handle processes where a single valve exhibits multiple nonlinearities (e.g., stiction and also an equal percentage valve characteristic) or where the various inputs exhibit different dynamics (e.g., one valve is sticky but another for the same process has linear dynamics) if the dynamics can be modeled and then included within the process-valve dynamic model.

The formulation of an MPC that includes the valve and process dynamics (Eqs. (7) and (8)) is as follows:

$$\min_{u_m(t)\in S(\Delta)} \int_{t_k}^{t_{k+N}} L_e(\tilde{q}(\tau), u_m(\tau))\, d\tau \tag{38a}$$

$$\text{s.t.} \quad \dot{\tilde{q}}(t) = f_q(\tilde{q}(t), u_m(t), 0) \tag{38b}$$

$$\tilde{q}(t_k) = q(t_k) \tag{38c}$$

$$\tilde{q}(t) \in Q_v, \ \forall\, t \in [t_k, t_{k+N}) \tag{38d}$$

$$u_m(t) \in U_m, \ \forall\, t \in [t_k, t_{k+N}) \tag{38e}$$

$$g_{\text{MPC},1}(\tilde{q}(t), u_m(t)) = 0, \ \forall\, t \in [t_k, t_{k+N}) \tag{38f}$$

$$g_{\text{MPC},2}(\tilde{q}(t), u_m(t)) \leq 0, \ \forall\, t \in [t_k, t_{k+N}) \tag{38g}$$

where the notation follows that in Eq. (11). The predicted process-valve state $\tilde{q}$ follows the model of Eqs. (38b) and (38c) and is bounded within the set Q_v (Eq. (38d); the set Q_v is defined to be the bounds on the process-valve model states, which may include, for example, the state constraints restricting $x \in X$ and the state constraints corresponding to $u_a \in U$ since u_a is a function of the states from Eq. (2) (since each $u_{m,i}$ is calculated by a state feedback controller) and Eq. (4). The constraints in Eqs. (38f) and (38g) may include constraints related to specific behavior of the valve. For example, in Durand and Christofides (2016), it is noted that a beneficial constraint for a sticky valve may be one which ensures that only physical values of the forces applied to the valve are predicted (for example, it may require the predictions $\tilde{P}$ of P to satisfy $\tilde{P} \geq 0$ for the tank level example). Theoretical results regarding disturbance rejection for an MPC with the form in Eq. (38) but with certain stability-related constraints added to the formulation have been developed in Durand and Christofides (2016). Guaranteed robustness to disturbances in that case requires several conditions to hold, including that the disturbance magnitude be sufficiently small. In general, there is no guarantee that the closed-loop response of a process under an MPC in the presence of disturbances will be as desirable as that in the case without disturbances.

Two potential limitations of an MPC for valve behavior compensation are: (1) The sampling period may, for computation time reasons, be significantly longer than the time that it takes for the forces on the valve to reach equilibrium after the deadband and stickband are overcome. This means that the MPC may not have the flexibility to change the force from the actuation rapidly in response to a rapid change of the friction force (this is discussed further in Section 5.4.2). (2) It may be difficult to determine all parameters of an appropriate first-principles model of the valve layer for a given valve (the valve layer for valve i is defined in this work to refer to all dynamics describing the relationship between $u_{m,i}$ and $u_{a,i}$, $i = 1, \ldots, m$). Empirical models for the valve layer dynamics (and potentially the process dynamics as well) may aid in handling both of these limitations because they may not require detailed information on the valve layer dynamics like the details of the friction force model or valve characteristic, and they may also be less stiff than a first-principles model (an example of this is demonstrated in Section 5.4.3), resulting in a lower computation time for the MPC for valve behavior compensation. If the model utilized within the MPC can capture the dominant process-valve dynamics to provide sufficiently accurate state predictions, it would be expected to be beneficial in compensating for stiction, even if it is not an exact model, due to the incorporation of state feedback. The following equation denotes an empirical model for use in the MPC-based valve behavior compensation method:

$$\dot{y}(t) = f_y(y, u_m) \tag{39}$$

where $y(t)$ is the predicted value of u_a from the empirical model at time t and has dynamics characterized by the vector function f_y. This empirical model can be used to predict the values of the process inputs in the objective function and constraints of Eq. (38a)(38) when a first-principles model is not used.

5.3. Valve behavior empirical modeling considerations following closed-loop dynamic analyses

Two questions that arise when considering how to empirically model a full process-valve system are: (1) what part of the process-valve dynamics should be captured in a single empirical model and (2) is it possible to develop empirical modeling strategies for valve behavior that are general rather than focused on a specific type of valve behavior. To explain the implications of the first question, we first examine stiction empirical modeling techniques in the literature (e.g., the Choudhury model (Choudhury et al., 2005), the Kano model (Kano et al., 2004), and the He model (He et al., 2007)), which generally assume that the relationship between u_a and the force applied to the valve is similar to that in Fig. 8, so they use an "if-then" (branched) type structure to mimic this (i.e., if the control signal has not changed enough to un-stick the valve, then the valve position does not change with a change in the control signal; if the control signal has changed enough to unstick the valve, the valve takes a new position defined by the empirical model). These models relate the valve position and the force on the valve determined by a controller. However, this may not eliminate the need to develop first-principles models for some of the dynamics relating $u_{m,i}$ and $u_{a,i}$ for the i-th valve. For example, if flow control is utilized on the valve as in the example of Fig. 7, some knowledge of the relationship between the valve output flow rate set-point from the major loop controller and the force applied to the valve by the minor loop controller is required to model the valve layer. If an equal percentage valve characteristic characterizes the $u_{a,i} - x_{v,i}$ relationship, the form of this model must be known. The principle demonstrated through this analysis is not specific to stiction: to avoid the need to obtain a first-principles model for any aspect of the valve layer dynamics, it may be beneficial to develop an empirical model that relates $u_{m,i}$ to $u_{a,i}$. We show in Section 5.4.3 that it may be possible to develop an acceptable relationship even when the $u_{m,i} - u_{a,i}$ dynamics are somewhat complex (e.g., they contain the dynamics not only of the valve but also of a flow controller for the valve).

If a $u_{m,i} - u_{a,i}$ relationship can be obtained, it should be determined whether it would be possible to obtain a $u_m - x$ relationship as well (i.e., to develop a single empirical model for the process-valve system that relates the controller output u_m to the process states such that it is not necessary to obtain data on the process input vector u_a when developing the empirical model). However, there may arise cases in which it may not be possible to easily capture the process and valve dynamics in the same empirical model. To see why difficulty may arise, consider a process with multiple inputs, all of which are adjusted by sticky valves. Because the valves are sticky, each change in $u_{m,i}$ will either cause $u_{a,i}$ to change appreciably (which will cause x to respond to the change in $u_{m,i}$), or it will not cause $u_{a,i}$ to change appreciably (which will cause x to continue behaving after the change in $u_{m,i}$ as if $u_{m,i}$ had not changed). Due to the coupling of the dynamics of the states of a process-valve system, the combination of $u_{a,i}$'s affects the process dynamics, so a branched empirical model describing the $u_m - x$ relationship may need to include different branches for every combination of sticking and slipping for all valves, which may lead to a difficult identification task. A solution if this is found to be an issue would be to empirically model each $u_{a,i} - u_{m,i}$ relationship for each valve as well as the $u_a - x$ relationship for the process (this may also be beneficial from a valve maintenance perspective because it permits monitoring of how closely $u_{a,i}$ matches $u_{m,i}$ for each valve (assuming that the $u_{a,i} - u_{m,i}$ relationship can be assessed frequently or potentially that an empirical modeling procedure for those dynamics could be automated), allowing valve maintenance to be performed first on those valves for which $u_{a,i}$ tracks $u_{m,i}$ the least).

To examine the implications of the second question above (whether a general empirical modeling strategy can be used to obtain the $u_{m,i} - u_{a,i}$ relationship) we return again to the stiction empirical models of the literature. Many of these assume that a specific trigger causes the valve to stick or slip and they assume a specific model for the valve response after slipping occurs that is related to the characteristics of the typical response of a sticky valve to control signal changes. For a general valve layer (i.e., the type of dynamics and control architecture within the valve layer are not specified), it is necessary to consider whether a $u_{a,i} - u_{m,i}$ relationship can be developed without necessarily knowing the underlying valve behavior/loop architecture represented through the relationship. Branched models may be required to do this because valves are not necessarily operated within a range of states throughout which linearization of the valve dynamics is adequate for representing the valve response. For example, consider the model of a valve's dynamics in Eqs. (27)–(32). The valve velocity must be forced through zero every time the direction of the valve movement changes, which is a point where Eq. (30) is non-differentiable due to the absolute value in the right-hand side. Therefore, the model of Eqs. (27)–(32) cannot be linearized at zero velocity every time the valve movement changes direction (which has the potential to be frequent). Though Eq. (30) represents the dynamics for only one of many friction models, its form indicates that the friction nonlinearity may need to be represented by more complex nonlinearities such as absolute values than are usually present in standard empirical model structures such as linear or polynomial state-space models, and as a result when the latter models are used, branched models may be required to capture the effects of the nonlinearities of the valves.

When a branched model is used, some understanding of the physics of the valve layer can be exploited by an engineer in developing the triggers for the branches, or attempts can be made to automate the determination of triggers from data. If the valve layer has a number of states, this may result in an empirical model with a significant number of branches and even with parameters that depend on the inputs to the valve layer. For example, consider that we want to develop an empirical model for the relationship between $u_{a,i}$ and $u_{m,i}$, $i = 1, \ldots, m$, when each $u_{m,i}$ is a valve output flow rate set-point from an MPC which is transmitted to a valve layer containing a sticky valve with a linear valve characteristic under a PI flow controller based on the error between $u_{m,i}$ and $u_{a,i}$. We assume that $u_{m,i}$, $i = 1, \ldots, m$, is held constant for a time period Δ during which the PI controller repeatedly computes new values of the pressure applied to the valve stem to drive $u_{a,i}$ to $u_{m,i}$. If the valve output flow rate set-point change direction reverses (e.g., the set-points $u_{m,i}$ were previously increasing but the next set-point is lower than the previous one), the valve may stick throughout some or all of the time period Δ during which $u_{m,i}$ is constant, depending on whether the pressure applied to the valve changes enough throughout Δ to overcome the force required to move the valve. Also, the PI controller will calculate larger control actions when the valve output flow rate set-point changes significantly (because this creates a large error between $u_{m,i}$ and $u_{a,i}$), and such larger control actions (pressures) are more likely to overcome the deadband/stickband within the time period Δ. Therefore, it is more likely that the valve will move if the controller is aggressively tuned or if the set-point change is large and the error between $u_{m,i}$ and $u_{a,i}$ affects the controller output. Saturation of the valve (e.g., the pressure from the pneumatic actuation drops to zero so that the valve can no longer move in the direction of decreasing pressure) can also occur. Therefore, the various branches of the response may need to be triggered by considerations related to the stiction dynamics and saturation of the pressure of the pneumatic actuation, with the time that the valve is stuck depending on the set-point change magnitude due to the flow controller. The procedure proposed for empirical modeling of the feedback loop for the sticky valve under consideration is as follows:

1. Collect valve layer input-output data (i.e., data relating $u_{a,i}$ and $u_{m,i}$, $i = 1, \ldots, m$), ensuring that data gathered represents all aspects of the valve layer response that should have separate equations (branches) within the piecewise model structure (e.g., sticking and slipping).
2. For each aspect of the response that requires its own model structure, select an appropriate structure based on the valve layer input-output data trends and determine what activates the different branches of the response (e.g., set-point change direction reversals).
3. Identify the parameters for the different branches of the model.
4. Develop models for any parameters that can be seen from the valve layer input-output data to be dependent on the valve layer inputs (e.g., parameters that depend on the magnitude of the valve output flow rate set-point change).
5. Validate the final piecewise-defined model.

It will be shown in Section 5.4.3 of this work that Step 2 in the procedure above may be able to be performed with standard empirical model structures in the chemical process industries, such as second-order or first-order-plus-dead time models (i.e., they do not take a form dependent on the valve behavior being modeled). Furthermore, the five steps above are general and therefore are not necessarily restricted to the valve layer with a sticky valve under flow control above but can be examined for extension to other control loop architectures and valve behavior that characterize the valve layer.

A final consideration related to empirical modeling of a process-valve system is that there may be states that it is desirable to constrain in an MPC-based valve behavior compensation strategy that would be known from a first-principles model but are not explicitly modeled within an empirical model. As a result, constraints of the MPC-based valve behavior compensation strategy may need to be adjusted to be in terms of the states of the empirical model and the inputs. For example, Eqs. (38f) and (38g) may include a constraint on the pressure from the pneumatic actuation to prevent it from saturating in the case that a sticky valve is in the loop. However, an empirical valve layer model relating $u_{m,i}$ to $u_{a,i}$ for a valve layer with a flow controller may not have any state related directly to this pressure. As a result, the following input rate of change constraints can be added to the MPC of Eq. (38a)(38) in place of Eqs. (38f) and (38g):

$$|u_{m,i}(t_k) - u^*_{m,i}(t_{k-1}|t_{k-1})| \leq \epsilon, \ i = 1, \ldots, m \tag{40a}$$

$$|u_{m,i}(t_j) - u_{m,i}(t_{j-1})| \leq \epsilon, \ i = 1, \ldots, m, \quad j = k+1, \ldots, k+N-1 \tag{40b}$$

These constraints require the differences between the values of $u_{m,i}$ at any two subsequent sampling periods of the prediction horizon to be no greater than ϵ and therefore can prevent large changes in the set-points $u_{m,i}$ between two sampling periods that may saturate the valve actuation (or wear the actuators (Durand et al., 2016)).

However, applying input rate of change constraints in an MPC for valve behavior compensation is not always beneficial. For example, consider the sticky valve without flow control of Eqs. (27)–(32). As exemplified in Fig. 5, the valve does not move when the valve is stuck if the change in u_m does not change the pressure applied to the valve enough to overcome the static friction force. This indicates that even if the valve dynamics were included in the MPC for valve behavior compensation for this valve

but input rate of change constraints were also included, the values of u_m that may satisfy these constraints may not differ enough from the values at the prior sampling time in some sampling periods to allow the valve to move. If the valve is under the flow controller of Eqs. (33) and (34), however, the pressure applied to the valve is not an explicit function of u_m, but instead is changed throughout a sampling period by the flow controller. If the difference between u_m and u_a in Eqs. (33) and (34) is large, it causes the pressure applied to the valve stem to change significantly, and may potentially cause the pressure applied by the actuation to saturate (e.g., hit its minimum bound) and therefore not allow the set-point u_m to be reached by u_a. In Eq. (38a)(38), this may be prevented through the actuation magnitude constraint; in the case when the empirical stiction model is used and details on the actuation magnitude are not captured by the empirical model so that they can be constrained, utilizing the input rate of change constraints may be beneficial for preventing large changes in u_m that could saturate the actuation and therefore prevent u_a from reaching u_m. This emphasizes that because stiction is a closed-loop effect, constraints added to an MPC to compensate for valve behavior should be chosen with an understanding of the impact of the controller and control loop architecture on the valve behavior.

Remark 6. Prior works that have looked at MPC with a general objective function with empirical models (Alanqar et al., 2017, 2015a,b) have focused on empirical models of the nonlinear process (rather than valves) and have indicated that significant computation time reductions may result from using empirical as opposed to first-principles models in MPC. We will demonstrate in Section 5.4.3 that empirically modeling the valve layer can result in computation time reduction even if the process is modeled with a first-principles model because it can make the process-valve combination model less stiff.

Remark 7. One could examine whether the MPC-based valve behavior compensation method, particularly with an empirical valve layer model, could be utilized for compensating for dynamic effects (e.g., slower movement of a valve or lack of movement) related to physical valve issues like oversizing, undersizing, corrosion, leaks through the valve packing, or diaphragm faults that can affect valve performance (Choudhury et al., 2008).

Remark 8. An appropriate empirical model structure for the valve layer input-output data must be selected. Many model identification techniques for obtaining linear and nonlinear empirical models exist that can be evaluated for their suitability for modeling a given valve layer input-output trend, which fall in the categories of state- space and input-output models (see, for example, (Ljung, 1999; Billings, 2013; Van Overschee and De Moor, 1996; Paduart et al., 2010)).

5.4. Valve behavior compensation methods: process examples

We now demonstrate the development and use of several of the valve behavior compensation methods described above for control loops containing sticky valves.

5.4.1. Level control example with a sticky valve: integral term modification

The process of Eq. (23) with the open-loop valve dynamics in Eqs. (27)–(32) was initially operated under the PI controller of Eqs. (24) and (25) for 15 600 s for a level set-point change from 0.5184 m to 0.15 m to reach q_l. Subsequently, it was controlled using the controller of Eqs. (36) and (37) (with $\hat{x} = h$) for a level set-point change from 0.15 m to 0.20 m. The explicit Euler method with a numerical integration step size of 10^{-5} s was used, and the results are shown in Fig. 9 (plotted every 100 000 integration steps) for

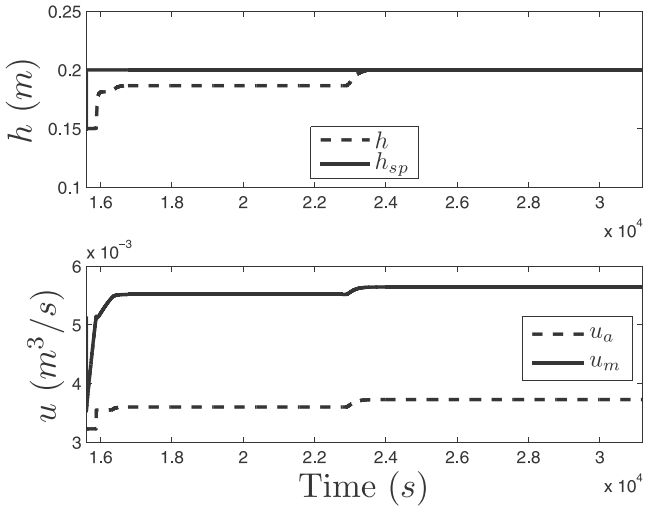

Fig. 9. Closed-loop trajectories of h, u_a, and u_m for the process of Eq. (23) under the controller of Eqs. (36) and (37) with $L = 7$ and $\beta = 0.007$, with the open-loop valve (Eqs. (27)–(32)), and $h_{sp} = 0.20$ m.

the case that $L = 7$, $\beta = 0.007$, and $t_{AW} = 22\,880$ s (i.e., 7280 s after the set-point change from 0.15 m to 0.20 m). From comparison with Fig. 4, the addition of the term containing L to the integral action was able to reduce control loop oscillations (though there is some offset from the set-point for the chosen L before t_{AW} because the integrator state in Eq. (37) can have $\dot{\zeta} = 0$ when $h \neq h_{sp}$). After t_{AW}, the value of u_m is able to change again because $\dot{\zeta}$ becomes nonzero, and eventually the valve moves and the forces due to this strategy balance in such a way that the set-point is achieved.

5.4.2. Level control example with a sticky valve: MPC with a first-principles valve layer model

For the level control problem, we develop an MPC for stiction compensation as follows:

$$\min_{u_m(t)\in S(\Delta)} \int_{t_k}^{t_{k+N}} Q_T (h_{\mathrm{sp}} - \tilde{h})^2 + R_T (u_{a,\mathrm{sp}} - \tilde{u}_a)^2 \, d\tau \tag{41a}$$

$$\text{s.t.} \quad \dot{\tilde{q}}(t) = f_q(\tilde{q}(t), u_m(t), 0) \tag{41b}$$

$$\tilde{q}(t_k) = q(t_k) \tag{41c}$$

$$0 \le \tilde{u}_a(t) \le 0.006, \ \forall\ t \in [t_k, t_{k+N}) \tag{41d}$$

$$0 \le u_m(t) \le 0.006, \ \forall\ t \in [t_k, t_{k+N}) \tag{41e}$$

$$\tilde{P} \ge 0, \ \forall\ t \in [t_k, t_{k+N}) \tag{41f}$$

where $u_{a,sp} = 0.00373$ m^3/s, $h_{sp} = 0.20$ m, $Q_T = 0.00001$, and $R_T = 1$. $\tilde{u}_a$ and $\tilde{h}$ denote the predictions of u_a and of the level according to Eq. (41b), respectively. The notation of Eq. (41a)(41) follows that in Eq. (38a)(38). The process-valve state vector $q^T = [h\ x_v\ v_v\ z_f]$ is modeled for the open-loop valve using Eqs. (23) and (27)–(32). The process-valve system was initiated at q_l. The level was controlled by the MPC of Eq. (41) for 150 s with $\Delta = 1$ s and $N = 50$. An integration step of 10^{-5} s was used within the MPC to integrate Eq. (41b), with an integration step of 10^{-6} s used outside

of the MPC to simulate the process. The constraints in Eqs. (41d) and (41f) were enforced once every sampling period. The objective function derivatives required by the optimization solver Ipopt were calculated using a centered finite difference, and the Ipopt limited-memory Hessian approximation option was used, so that the non-differentiability in Eq. (30) did not prevent a solution to the optimization problem from being obtained. The results in Fig. 5 (designated by C because the valve dynamics are compensated) are plotted every 1000 integration steps and indicate that the MPC including the valve dynamics drove the level toward its set-point, in contrast to the MPC that did not include the actuator dynamics (designated by U in this figure). The reason for this is that the MPC of Eq. (41a)(41) incorporates the full process-valve model, and thus computes an input trajectory that accounts for the manner in which the forces on the valve will balance under the control actions calculated by the MPC.

Though the MPC was able to drive the level toward its set-point (a significant improvement with regard to set-point tracking of the level compared to the case that the valve dynamics were not accounted for within the MPC), the fact that the valve is operated without flow control reduces the flexibility of the MPC to be able to maintain the level at the set-point for all times after it first approaches the set-point in Fig. 5. Specifically, each time that the MPC sets u_m, the pressure applied to the valve changes according to the relationship of Eq. (32) since the valve is operated without flow control. However, because the MPC implements piecewise-constant control actions that are held for a sampling period, the pressure that is applied to the valve (a function of u_m calculated by the MPC) is held constant throughout a sampling period. The length of the sampling period in this example is long compared to the dynamics of the valve, such that the dynamics of the valve under a constant applied pressure dictate the final position of the valve at the end of a sampling period. The result is that the MPC is not able to find a value of u_m that will drive the valve, subject to its dynamics during the sampling period that the pressure is held constant and the MPC cannot intervene, exactly to the valve position corresponding to the steady-state flow rate through the valve when the level set-point is achieved. Instead, the MPC must continuously calculate new values of u_m that allow the valve to stick and slip in ways that the MPC finds will minimize the tracking objective function and therefore keep the value of h in a region around the set-point over time. Based on this analysis, potential ways of improving the set-point tracking of the level include decreasing the MPC sampling period until it is on a time scale comparable to the time scale of the valve dynamics, increasing the prediction horizon to give the MPC greater foresight to potentially allow it to determine a sequence of values of u_m that can drive the value of u_a to its set-point, or adding flow control to the valve and then including the dynamics of both the valve and the flow controller in the MPC as it calculates set-points u_m for the flow controller.

Remark 9. Fig. 5 demonstrates the effects of not accounting for the behavior of the valve of Eqs. (27)–(32) within an MPC (no significant change of the level for certain changes in the valve output flow rate set-point u_m) and the improvement that can be obtained when the dynamics are accounted for. However, other types of valve behavior that are not exhibited by the valve of Eqs. (27)–(32) can result in different types of negative effects when the valve behavior is not included within the MPC model for making state predictions. For example, consider a valve without stiction but with the following equal percentage valve characteristic (Coughanowr and LeBlanc, 2009):

$$u_a = u_{a,\max} e^{\ln(0.03) x_v / x_{v,\max}} \tag{42}$$

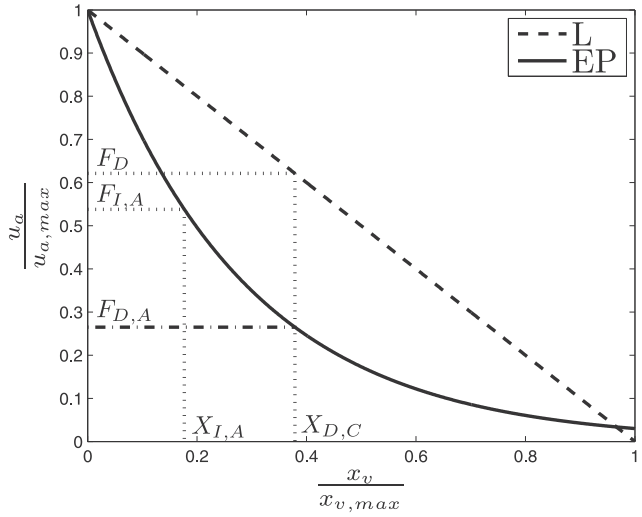

Fig. 10. Figure depicting linear (L) and equal percentage (EP) valve characteristics of Eqs. (32) and (42), respectively, along with several fractions of the maximum flow rate ($F_{I,A} = 0.5379$, $F_D = 0.62113$, and $F_{D,A} = 0.2649$) and of the maximum stem position ($X_{I,A} = 0.1768$ and $X_{D,C} = 0.37887$) for the level control example.

developed for the case that the valve stem is fully retracted when the valve is fully open and is fully extended when the valve is fully closed. Assume that the valve can be manipulated in such a manner that the valve position is an explicit function of u_m given by Eq. (31) (i.e., $x_v = x_{v,\max} - \frac{u_m}{u_{a,\max}} x_{v,\max}$) though this linear relationship does not reflect the nonlinear $x_v - u_a$ relationship of Eq. (42). If an MPC is used to control the process but is not aware of the mismatch between the valve behavior of Eq. (42) and the linear $u_m - x_v$ relationship that sets the valve position (a similar concept to the mismatch between Eq. (32) and the actual $u_a - P$ relationship for the sticky valve of Eqs. (27)–(31)), permanent offset of the level from its set-point can result due to the plant-model mismatch. For example, consider again the set-point change from an initial level of 0.15 m, corresponding to a steady-state flow rate of 0.00323 m^3/s, to the set-point h_{sp} = 0.20 m corresponding to $u_{a,sp}$ = 0.00373 m^3/s. The steady-state flow rate for a level of 0.15 m corresponds to a fraction $F_{I,A}$ = 0.5379 of the maximum flow rate of 0.006 m^3/s through the valve as shown in Fig. 10. For the equal percentage valve of Eq. (42), the valve position associated with the steady-state flow rate for the initial level is a fraction $X_{I,A}$ = 0.1768 of its maximum. When the set-point of the level is changed to 0.20 m, the flow rate out of the valve should increase to achieve this (ideally it should reach the fraction of the maximum flow rate F_D = 0.62113 shown Fig. 10). For the equal percentage valve of Eq. (42), this flow rate is achieved at a fraction of 0.1358 of the maximum stem position. The $u_m - x_v$ relationship used to set the stem position based on x_v, however, is linear, so when the MPC requests that $u_m = u_{a,sp}$, the linear $u_m - x_v$ relationship moves the valve stem to a position corresponding to a fraction $X_{D,C}$ = 0.37887 of the maximum stem position. However, when the fraction of the stem position for an equal percentage valve is 0.37887, the fraction of the maximum flow through the valve is $F_{D,A}$ = 0.2649 (corresponding to a flow rate lower than the initial value instead of above it as desired). This example highlights that including valve behavior in MPC can be beneficial for many types of valve behavior. Also, the example valve in this section has a $u_m - u_a$ relationship of the form in Eq. (2) since x_v in the linear $u_m - x_v$ relationship can be substituted in terms of u_m in the $u_a - x_v$ relationship of Eq. (42).

Table 2
Ethylene oxidation model parameters.

Parameter	Value
γ_1	−8.13
γ_2	−7.12
γ_3	−11.07
A_1	92.80
A_2	12.66
A_3	2412.71
B_1	7.32
B_2	10.39
B_3	2170.57
B_4	7.02

5.4.3. Ethylene oxidation example with a sticky valve: MPC with an empirical valve layer model

In this section, we return to the ethylene oxidation example of Section 4.2 for the case that $u_{a,2} = 0.5$ and $u_{a,3} = 1.0$ (the values of the other parameters are listed in Table 2). We consider that the value of $u_{a,1}$ is adjusted by a spring-diaphragm sliding-stem globe valve (because it is the only manipulated input considered for this process in the following example, we will drop the "1" in the subscript for this section and refer to the process input as "u_a"). This valve is under flow control and has the same design as the sticky valve described in Section 4.1 (i.e., it is pneumatically actuated and pressure-to-close, with no pressure applied to the valve initially when it is in its fully open position, it has $x_v = 0$ m when the valve is fully open and $x_v = x_{v,\max} = 0.1016$ m when the valve is fully closed with $u_a = 0$, and the valve layer dynamics are described by Eqs. (27)–(31), (33) and (34)) except that the time unit for all parameters and variables is denoted by a dimensionless unit t_d instead of s for consistency with the dimensionless units in Eq. (35a)(35) (i.e., all valve model parameter values in Table 1 apply for this valve except that each instance of the unit s in that table is replaced with t_d in this example) and the fully open valve position corresponds to $u_a = u_{a,\max} = 0.7042$. The values of ζ_P and of the steady-state value of the pressure P_s are re-set each time that u_m changes (ζ_P is re-set to zero, and P_s is set to the last applied pressure). The value of u_m is changed by an EMPC (an MPC with an economics-based objective function) every sampling period of length $\Delta = 0.2\ t_d$.

The control objective is to maximize the yield of ethylene oxide utilizing an MPC that accounts for the valve dynamics, where the yield is given by the following ratio of the amount of ethylene oxide produced from the reactor in a time period of length $t_f - t_0$ to the amount of ethylene fed to the reactor in that time:

$$Y(t_f) = \frac{\int_{t_0}^{t_f} u_a(\tau)x_3(\tau)x_4(\tau)d\tau}{\int_{t_0}^{t_f} 0.5u_a(\tau)d\tau} \tag{43}$$

We also consider that the valve output flow rate is constrained between the minimum flow through the valve (0) and the maximum flow (0.7042), and is also required to satisfy the following restriction on the amount of ethylene that can be fed in a time period of length $t_f - t_0$:

$$\frac{1}{t_f - t_0}\int_{t_0}^{t_f} 0.5u_a(\tau)d\tau = 0.175 \tag{44}$$

This constraint requires that the amount of ethylene fed to the process in a time period of length $t_f - t_0$ must equal the amount that would be fed in that time period under steady-state operation. We seek to avoid fully closing the valve by requiring the MPC to keep the value of u_m between 0.0704 and 0.7042.

To achieve the control objectives, we will utilize an MPC with an empirical model of the valve dynamics, and we will compare the computation time of that controller with the computation time of an MPC that includes a first-principles model of the valve dynamics. We develop the empirical model for the valve layer described in Eqs. (27)–(31), (33) and (34) according to the steps outlined in Section 5.3. According to Step 1, we first gather $u_m - u_a$ data, and notice that when the set-points repeatedly change in the same direction, the valve responds rapidly to the set-point change, but when the set-point change direction reverses, there is a delay before the valve responds. Also, there is a greater delay for small set-point changes than for large set-point changes when the deadband is encountered due to the use of the PI controller in the valve layer. In addition, the valve layer input-output data indicates that when the valve output set-point is kept constant for multiple sampling periods, the valve output will not exhibit deadband if the next change in the set-point is in the same direction as the changes prior to the valve set-point remaining constant, but will exhibit deadband if the next change in the set-point is in the opposite direction to the last changes. The valve layer data also suggests that valve output flow rates above about 0.5164 are not achievable with the pressure available from the pneumatic actuation after the valve first begins to close because stiction alters the $u_a - P$ relationship such that these flow rates would require negative pressures to be reached (i.e., since the valve is initialized with $u_a = 0.7042$, it can only close (it cannot reverse direction to open more) until $u_a \sim 0.5164$, and subsequently cannot reach flow rates above that value).

The above observations are used in Step 2 of the model identification procedure to postulate that the dynamics between u_a and u_m can be captured in a piecewise-defined model with two branches, one corresponding to the response of u_a when the set-point changes in u_m are repeatedly in the same direction (no deadband), and another corresponding to the response when the set-point changes switch direction (deadband), with a special consideration for the case that the set-point does not change between two sampling periods. The part of the model corresponding to the case when there is deadband before the valve moves should have different speeds of response of the valve for different set-point change magnitudes. The valve layer input-output data should be gathered while avoiding increasing the set-point u_m above 0.5164 to avoid gathering data for flow rates where the pressure is saturated (the decision was made not to add branches to the empirical model to account for saturation of the actuation pressure due to the complexity that this adds to the empirical model, but to instead seek to avoid saturating the pressure during process operation by utilizing the input rate of change constraints of Eq. (40a)(40) in the MPC used to control the process).

Step 3 of the model identification procedure will now be carried out to identify the equations for the two branches of the proposed model. We first verify that such a piecewise-defined valve layer model is necessary by showing the results of attempting to identify a single model for the valve layer based on the valve layer input-output data. The valve layer input-output data was gathered by initializing the valve at its fully open position ($u_a = 0.7042$, $P_s = 0\text{kg/m}.t_d^2$, $\zeta_P = 0$, $z_f = 0$ m, $x_v = 0$ m, $v_v = 0\text{m}/t_d$) and integrating the first-principles valve layer model in Eqs. (27)–(31), (33) and (34) with the explicit Euler numerical integration method and an integration step of $h_I = 10^{-6}\ t_d$ for 19 step changes in the set-point (the set-point was first decreased from $u_m = 0.7042$ to 0.7, and was subsequently decreased to 0.15 in increments of 0.05, and then increased to 0.5 in increments of 0.05, with each set-point held for a sampling period). A subset of the $u_m - u_a$ data generated is shown in Fig. 11. Based on the data generated, the valve output response to a set-point change was postulated to be able to be described by a second-order linear dynamic model. The values of u_m and u_a were measured every 10^{-4} time units (every 100 integration steps; i.e., $\Delta_e = 10^{-4}\ t_d$), and the following ARX model

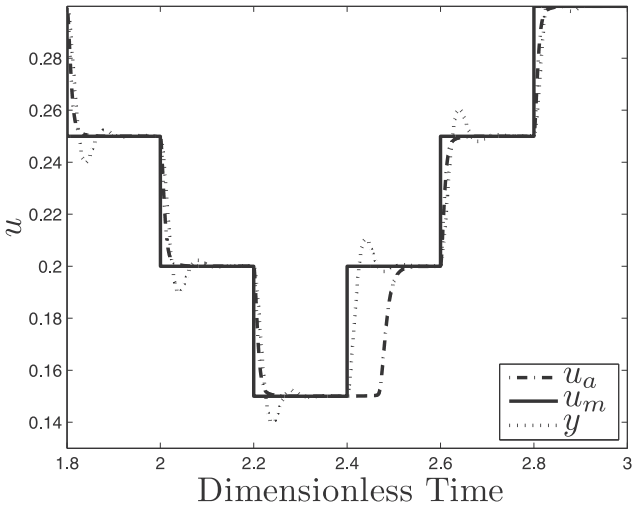

Fig. 11. Comparison of valve layer set-point (u_m), valve layer output (u_a), and prediction of the valve layer output (y) from Eq. (45) when 19 set-point changes are applied (a subset of the data is shown).

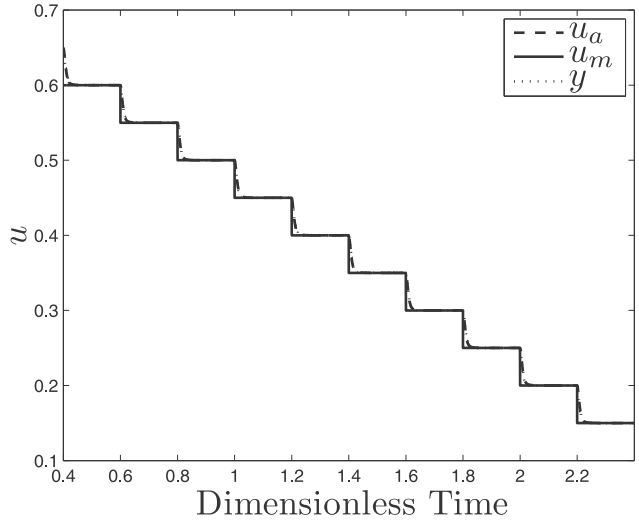

Fig. 12. Comparison of valve layer set-point (u_m), valve layer output (u_a), and prediction of the valve layer output (y) using the set-points decreasing between 0.6 and 0.15 and Eq. (46) (y overlays u_a).

was fit to the data by using a least-squares regression:

$$y(\tilde{t}_j) = 1.99212y(\tilde{t}_{j-1}) - 0.99219y(\tilde{t}_{j-2}) + 0.00035u_m(\tilde{t}_{j-1}) - 0.00027u_m(\tilde{t}_{j-2}) \quad (45)$$

where $y(\tilde{t}_j)$ refers to the predicted value of u_a for the jth measurement of the valve layer output data (i.e., at time $\tilde{t}_j$). When the predictions y are generated from this model and the input data, they overshoot the values of u_a, and there is poor agreement with u_a when the valve velocity changes sign (deadband is reached), as shown in Fig. 11.

Though it was not possible to identify an adequate second-order model using the input- output data for the entire set of 19 set-point changes, it is possible to successfully identify a second-order model if only the data corresponding to the set-point decreases between 0.6 and 0.15, for which no deadband occurs, is used to identify the model. In this case, the following model is obtained:

$$y(\tilde{t}_j) = 1.96209y(\tilde{t}_{j-1}) - 0.96249y(\tilde{t}_{j-2}) + 0.00038u_m(\tilde{t}_{j-1}) + 0.00002u_m(\tilde{t}_{j-2}) \quad (46)$$

When the decreasing set-points between 0.6 and 0.15 are used as inputs in Eq. (46), the predictions y of the valve output closely match the actual values, as shown in Fig. 12.

To complete Step 3 of the empirical modeling procedure, it necessary to complement Eq. (46) with a model for the case that deadband is observed. Based on the valve layer input-output data in Fig. 11 corresponding to the deadband when u_m changes from 0.15 to 0.2, it is postulated that the response of the valve output to set-point change direction reversals can be modeled as a first-order process with time delay. However, the values of the time constant τ and of the delay α in such a model are dependent on the magnitude of the set-point changes because the speed of the response of the valve layer to a set-point change in u_m depends on the magnitude of the set-point change. Closed-loop simulations indicate that for a set-point change direction reversal, set-point changes less than approximately 0.02 are unable to cause the PI controller to overcome the deadband within a sampling period. To determine the dependence of the delay on the magnitude of the set-point change, in accordance with Step 4 of the model identification procedure, u_m was decreased from 0.7042 to 0.15, and subsequently u_m was increased by set-point changes of different magnitudes. The regression method in Ogunnaike and Ray (1994) for the determination of the parameters of a first-order-plus-dead-time model was applied to the data generated for each set-point change. A plot of the resulting delays against the set-point changes with which they were associated was fit to the function a/x using the MATLAB function lsqcurvefit, with $a = 0.0037$ providing the best fit. The values of τ associated with each delay were averaged to give $\tau = 0.0123$ for the first-order-plus-dead-time model. Thus, the first-order-plus-dead-time model is written in discrete-time form as:

$$y(\tilde{t}_j) = \begin{cases} y(\tilde{t}_{j-1}), \ \tilde{t}_j - t_k < \alpha \\ y(t_k) + \exp(-\Delta_e/\tau)(y(\tilde{t}_{j-1}) - y(t_k)) \\ \quad +K(1 - \exp(-\Delta_e/\tau)) \\ \times(u_m(t_k) - u_m(t_{k-1})), \ \tilde{t}_j - t_k \geq \alpha \end{cases} \quad (47)$$

where

$$\alpha = \begin{cases} \Delta, \ |u_m(t_k) - u_m(t_{k-1})| < 0.02 \\ a/(|u_m(t_k) - u_m(t_{k-1})|), \ |u_m(t_k) - u_m(t_{k-1})| \geq 0.02 \end{cases} \quad (48)$$

In Eqs. (47)– (48), k is the value of k that brings t_k closest to $\tilde{t}_j$ ($t_k \leq \tilde{t}_j$), and $K = 1$.

Incorporating the above considerations, the following discrete-time empirical valve layer model was devised and validated to perform well for a number of valve layer input-output data points, completing Step 5 of the model identification procedure:

1. If the set-point has not changed between t_k and t_{k-1} and also did not change between t_{k-1} and t_{k-2}, set $y(t) = y\ (t_k)$ for all $t \in [t_k, t_{k+1})$.
2. If two set-point changes are in the same direction, or if the set-point has been constant for some time but has now changed in the same direction that it was changing prior to becoming constant, use the model of Eq. (46).
3. If two set-point changes are in opposite directions, or if the set-point has been constant for some time but has now changed in the opposite direction to that in which it was changing prior to becoming constant, use the model of Eqs. (47) and (48).

The MPC-based stiction compensation strategy incorporating the empirical model described above is as follows:

$$\min_{u_m(t)\in S(\Delta)} \int_{t_k}^{t_{k+N_k}} -y(\tau)\tilde{x}_3(\tau)\tilde{x}_4(\tau)\ d\tau \quad (49a)$$

$$\text{s.t.} \ \ \dot{\tilde{x}}(t) = f(\tilde{x}(t), y(t), 0) \quad (49b)$$

$$\dot{y}(t) = f_y(y, u_m) \tag{49c}$$

$$\tilde{x}(t_k) = x(t_k) \tag{49d}$$

$$y(\tilde{t}_0) = u_a(t_0) \tag{49e}$$

$$0.0704 \le u_m(t) \le 0.7042, \ \forall\, t \in [t_k, t_{k+N_k}) \tag{49f}$$

$$0 \le y(t) \le 0.7042, \ \forall\, t \in [t_k, t_{k+N_k}) \tag{49g}$$

$$|u_m(t_k) - u_m^*(t_{k-1}|t_{k-1})| \le 0.1 \tag{49h}$$

$$|u_m(t_j) - u_m(t_{j-1})| \le 0.1, \ j = k+1, \ldots, k+N_k-1 \tag{49i}$$

$$\int_{t_k}^{t_{k+N_k}} y(\tau)d\tau + \int_{(p-1)t_p}^{t_k} u_a^*(\tau)d\tau = 0.175t_p/0.5 \tag{49j}$$

where the notation follows that in Eqs. (11a)(11) and (38a)(38). The notation $u_m^*(t_{k-1}|t_{k-1})$ signifies the value of u_m that was determined to be optimal at the prior sampling time and was applied to the process for the sampling period between t_{k-1} and t_k. Minimization of the objective function in Eq. (49a) maximizes the yield of ethylene oxide when the amount of reactant fed to the process over the $p-th$ operating period of length $t_p = 1\ t_d$ meets the constraint in Eq. (49j) (the notation $u_a^*(t)$ signifies a value of u_a that was applied to the process at a past time t). Enforcing the constraint of Eq. (49j) ensures that Eq. (44) is satisfied by the final time t_f of operation. Two operating periods were simulated under this EMPC; though a longer simulation may reduce the effects from the transient on the results, the two operating periods simulated are sufficient for demonstrating that an empirical model of the valve dynamics can readily be used in place of a first-principles model in the MPC for valve behavior compensation. A shrinking prediction horizon N_k was used in each operating period with an initial length of 5 at the beginning of each operating period. At each subsequent sampling time, the prediction horizon was decreased by 1. The process model of Eq. (49b) (which is the model of Eq. (35a)(35) with the single input $u_{a,1}$ as mentioned above) is integrated using the explicit Euler numerical integration method with an integration step size of $h_{emp} = 10^{-4}\ t_d$ for making state predictions.

Eq. (49c) signifies that the predictions y of u_a in the EMPC come from the empirical model developed in this section. Eq. (49c) is written in continuous-time form for consistency with the remainder of the manuscript in which a continuous-time model of the process-valve dynamics is utilized (in the sense that differential equations are considered to constitute the process model, though their solution must be obtained through numerical discretization because no analytic solution is available), though the results presented for this example come from utilizing the discrete-time empirical valve layer model developed in this section. Because both the numerically discretized (with explicit Euler) continuous-time process dynamic model and the empirical valve layer model evolve every $10^{-4}\ t_d$ when state predictions are made within the EMPC (i.e., $\Delta_e = h_{emp}$), the discrete-time nature of the empirical model poses no issues for combining it with the continuous-time process model for making state predictions. In the simulations, the value of y was not updated with a state measurement of u_a at each sampling time but instead evolved in an open-loop fashion

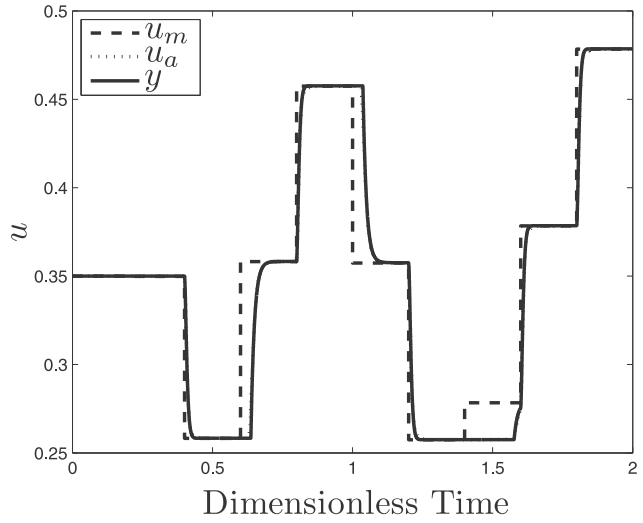

Fig. 13. Comparison of valve layer set-point (u_m), valve layer output (u_a), and prediction of the valve layer output (y) under the EMPC using an empirical valve layer model (y almost overlays u_a).

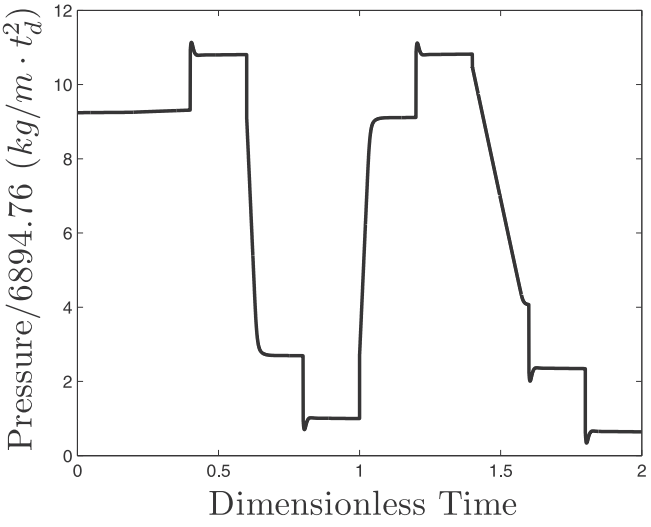

Fig. 14. Pressure applied to the valve when the EMPC using an empirical valve layer model is used.

(the notation in Eq. (49e) signifies that the initial data required for simulating the valve layer based on the empirical model (i.e., $y(\tilde{t}_0)$ and $y(\tilde{t}_{-1})$) are known and used to integrate the empirical model for all times without feedback of u_a). The state constraint in Eq. (49g) was enforced every integration step. The input rate of change constraints in Eqs. (49h)–(49i) are added to reduce the likelihood that the EMPC will request unreachable flow rates that would cause the pressure from the pneumatic actuation to become saturated at zero. The optimization problems were solved using the open-source interior-point optimization solver Ipopt (Wächter and Biegler, 2006) with a tolerance of 10^{-10}.

Fig. 13 shows the trajectories of u_a, u_m, and y initiated from $[x_1\ x_2\ x_3\ x_4\ x_v\ v_v\ z_f\ \zeta_P] = [0.997\ 1.264\ 0.209\ 1.004\ 0.051\ m\ 2.000 \times 10^{-6}\ m/t_d\ 1.426 \times 10^{-5}\ m\ 0]$ resulting from the use of the empirical EMPC. The empirical model was successfully able to capture the behavior of u_a, and the EMPC calculated set-points that the valve layer could track. Fig. 14 shows the pressure applied to the valve throughout this closed-loop simulation, which avoided saturating at zero with the help of the input rate of change

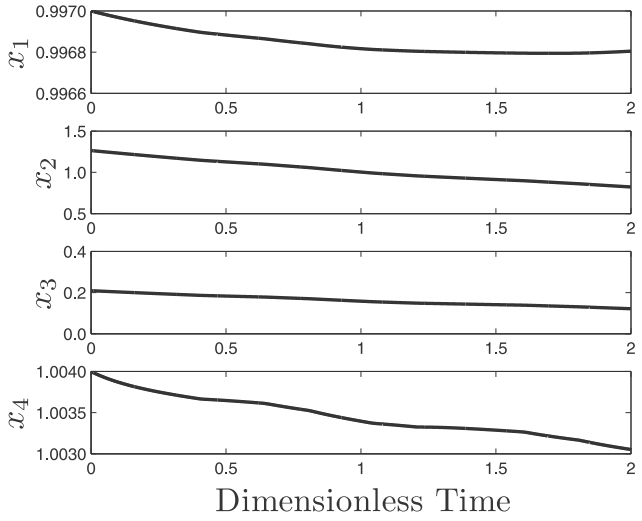

Fig. 15. Closed-loop process states under the EMPC using an empirical valve layer model.

constraints. Fig. 15 shows the closed-loop process states under the empirical EMPC.

In addition to calculating reachable set-points and preventing pressure saturation in the two operating periods simulated, the MPC-based valve behavior compensation strategy with an empirical model was also able to ensure that the integral material constraint was not significantly violated. In the first operating period, the empirical EMPC used only 0.02% less material than required by the material constraint, and in the second operating period only 0.05% less.

A comparison of a simulation of the form of Eq. (49a)(49) but with the first-principles valve layer model of Eqs. (27)–(31), (33) and (34) in place of the empirical model of Eqs. (46)–(48) was formulated, in which the first-principles model was simulated with an integration step of 10^{-5} t_d within the MPC, and state feedback of the process- valve states was obtained at each sampling time. This integration step size is smaller than for the simulation with the empirical EMPC because the first-principles model of Eqs. (27)–(31), (33) and (34) cannot be integrated with a step size of 10^{-4} t_d using explicit Euler due to numerical stability issues (i.e., the simulation does not produce numerical results within a reasonable range, which occurred for some smaller integration step sizes as well). The constraint of Eq. (49g) was enforced on u_a every 10 integration steps so that it was enforced every 10^{-4} t_d as for the empirical EMPC. The finite difference approximation used for the gradients of the objective function and constraints used a perturbation one order of magnitude smaller than in the empirical EMPC. The resulting simulation of two operating periods took approximately three times longer to solve than the MPC of Eq. (49a)(49) where the integration step within the MPC was 10^{-4} t_d. Though the difference in computation time depends on a large number of factors such as the code used and the integration step size, it is significant that the empirical model is less stiff than the first-principles model.

Remark 10. The computation time comparison is not meant to be an exact numerical comparison because it is difficult to determine the exact minimum step size that can be utilized within the first-principles EMPC for comparison with the computation time of the empirical EMPC. Therefore, we do not focus on providing exact computation time results, but instead highlight the difference in stiffness of the models, which is demonstrated in that an integration step size smaller than that of the empirical model must be utilized to integrate the first-principles model. In general, a less stiff model is considered to have the potential to be more computationally efficient, and through the example, we show that empirical modeling of a valve layer has the potential to develop a more computationally tractable model of the valve layer than would be obtained from first-principles. We do not consider implicit numerical integration methods instead of explicit methods because they are harder to implement. MPC's need to be solved on-line within a sampling period, and the numerical integration is performed many times to simulate the process throughout the prediction horizon at every iteration of the numerical optimization method. Therefore, a simple implementation of numerical integration is desirable.

6. Perspectives on valve nonlinearity compensation

A conclusion of the results in this work is that an MPC design that utilizes models of both the process and valve behavior for making state predictions provides a systematic method for driving an output to its set-point that can account for multivariable interactions in a process-valve dynamic system and constraints such as valve output and actuation magnitude saturation that can lead to undesirable closed-loop behavior. This method is not restricted to linear plant dynamics, and it does not require tuning of compensator-specific parameters that are not clearly tied to the process output responses as do some of the stiction compensation methods discussed above such as flow control, the integral term modification method, and knocker-type methods. The benefits of an MPC including valve dynamics for improving the issues commonly observed due to valve behavior indicate that it may be beneficial for industry to consider wider use of MPC due to analysis not only of whether the chemical process itself would benefit from being controlled by an MPC (which is the typical analysis performed), but also of whether it might provide better valve behavior compensation in the long run (undesirable behavior like valve stiction can develop over time) that may reduce efficiency and profit in the long-term and therefore make MPC a more attractive option than classical regulatory control designs. Thus, more analysis of the impact of actuator dynamics at the initial design phase may allow for better controller designs to be chosen that can handle changes in the actuator dynamics that often plague processes at a later phase and are less straightforward to handle when non-model-based control strategies are attempted to be used to handle nonlinear valve behavior.

Though the MPC-based valve behavior compensation method was shown in the process examples in this work to be beneficial at compensating for valve behavior, it was also shown that it has limitations in handling valve nonlinearities. For example, in Section 5.4.2, it was noted that a valve without flow control under MPC accounting for valve stiction may not be able to keep a process output at its set-point for all times when the MPC sampling period is long compared to the time scale of the valve dynamics such that the MPC is not able to regularly adjust the force applied by the valve actuation throughout a sampling period. An alternative to this is to use a flow controller for the valve or a small sampling period for the MPC to allow the force from the valve actuation to be adjusted frequently as the valve position changes according to its dynamics to try to drive it to the position corresponding to the valve output set-point. However, this may cause significant variations in the valve actuation during the time that the valve position is being adjusted, which may increase actuator wear (Ivan and Lakshminarayanan, 2009). This indicates that an MPC-based valve behavior compensation method must seek to balance actuator wear and set-point offset for certain control architectures and valve nonlinearities through appropriate constraints and design of parameters such as the sampling period. Another conclusion of this work is that because the effects observed in sticky control loops are closed-loop effects, changing the control design of a system

may result in different process output responses in a control loop in which valve dynamics cannot be neglected. This is important to consider as controllers at a plant are re-tuned or as upgrades are made to the control design.

Finally, the closed-loop perspective on valve behavior developed in this work can impact the stiction detection and quantification literature. It gives greater insight into the benefits and limitations of the detection/quantification methods for stiction in the literature, which are reviewed in Brásio et al. (2014) and include shape-based methods and model identification-based methods. Many of the shape-based methods (e.g., Horch, 1999; Choudhury et al., 2006; Singhal and Salsbury, 2005; Srinivasan et al., 2005a) assume that a specific pattern exists in the data from the measured outputs of the system (process outputs or valve outputs), often in relation to the controller outputs. It has been highlighted that the process and controller dynamics will affect the patterns and thus may reduce the effectiveness of shape-based methods (e.g., He et al., 2007 notes that the stiction detection method in Horch (1999) may give different results depending on the controller tuning, and Choudhury et al. (2006) and Jelali and Huang (2010) also note that the pattern-based methods are not always effective because patterns depend on the controller, process, and valve dynamics). The present manuscript gives a general mathematical framework for analyzing the difficulties noted with pattern- based methods through a process-valve dynamic model. It also gives greater insight into the conditions under which the assumption that oscillations are occurring in a process output due to stiction may not hold (e.g., when the controller, process, and valve dynamics produce the uncompensated case in Fig. 5). Multiple model identification-based stiction detection/quantification methods (see, for example, Srinivasan et al. (2005b); Jelali and Huang (2010); Jelali (2008)) assume that the process can be described by a linear model, which may be a limiting assumption especially as the requirement of steady-state operation is being challenged by the recent developments in EMPC (Ellis et al., 2014a).

The primary goal of stiction detection methods is to identify problematic valve behavior so that maintenance can be performed on a valve, and quantification methods are intended to be used to prioritize valve maintenance based on which valves are most sticky. The empirical modeling strategy in this work could be considered as a valve behavior detection/quantification strategy that is not limited to stiction. The $u_{m,i} - u_{a,i}$ relationship could be developed for every valve if $u_{m,i} - u_{a,i}$, $i = 1, \ldots, m$, data is available. The difference between $u_{m,i}$ and $u_{a,i}$ could then be tracked over time, and when it becomes significant, the valve could be flagged for maintenance. The valves for which $u_{a,i}$ deviates most significantly from $u_{m,i}$ could be given priority in the maintenance schedule. Though measurements of flow through a valve ($u_{a,i}$) are not always available in industrial applications when the control loop is not a flow control loop (Thornhill and Horch, 2007), this analysis indicates that new instrumentation to provide measurements of process variables such as flow (when it is not already measured) may be beneficial long-term for detecting and compensating for valve behavior by allowing empirical models to be developed for a process-valve system when it may be difficult to obtain a process-valve model without the flow measurement (Section 5.3).

A final observation is that many contributions to the stiction literature have focused on stiction as the nonlinearity in the process-valve system (i.e., many works examine linear processes and linear controllers); the results of this work indicate that nonlinear processes, especially with multiple inputs all affected by nonlinear valve behavior, may be particularly interesting to consider in future works on stiction detection, quantification, and compensation, due to the multivariable interactions of the process-valve states, which may, as noted above, best be handled with multiple-input/multiple-output nonlinear control designs.

7. Conclusions

In this work, we analyzed the roles of the process, valve, and controller dynamics, and also the control loop architecture, in the closed-loop response of a process-valve dynamic system. The closed-loop perspective discussed allows a variety of valve behaviors (e.g., linear valve dynamics and stiction) to be analyzed within a single framework. It was demonstrated to be useful for explaining how a number of stiction compensation methods from the literature seek to compensate for stiction at a fundamental mathematical level, and also was shown to be beneficial for developing new valve behavior compensation techniques such as an integral term modification stiction compensation method and an MPC design incorporating a dynamic model (first-principles or empirical) of the full process-valve system. A level control example and a continuous stirred tank reactor were used to demonstrate the concepts discussed throughout the manuscript.

Acknowledgements

Financial support from the National Science Foundation and the Department of Energy is gratefully acknowledged.

References

Alanqar, A., Durand, H., Christofides, P.D., 2015a. On identification of well-conditioned nonlinear systems: application to economic model predictive control of nonlinear processes. AIChE J. 61, 3353–3373.
Alanqar, A., Durand, H., Christofides, P.D., 2017. Error-triggered on-line model identification for model- based feedback control. AIChE J. 63, 949–966.
Alanqar, A., Ellis, M., Christofides, P.D., 2015b. Economic model predictive control of nonlinear process systems using empirical models. AIChE J. 61, 816–830.
Alfani, F., Carberry, J.J., 1970. An exploratory kinetic study of ethylene oxidation over an unmoderated supported silver catalyst. La Chimica e L'Industria 52, 1192–1196.
Amrit, R., Rawlings, J.B., Angeli, D., 2011. Economic optimization using model predictive control with a terminal cost. Annu. Rev. Control 35, 178–186.
Armstrong-Hélouvry, B., Dupont, P., Canudas De Wit, C., 1994. A survey of models, analysis tools and compensation methods for the control of machines with friction. Automatica 30, 1083–1138.
Bacci di Capaci, R., Vaccari, M., Pannocchia, G., 2017. A valve stiction tolerant formulation of MPC for industrial processes. In: Proceedings of the 20th IFAC World Congress, Toulouse, France. Toulouse, France, pp. 9374–9379.
Billings, S.A., 2013. Nonlinear System Identification: NARMAX Methods in the Time, Frequency, and Spatio-temporal Domains. John Wiley & Sons, Chichester, West Sussex.
Brásio, A.S.R., Romanenko, A., Fernandes, N.C.P., 2014. Modeling, detection and quantification, and compensation of stiction in control loops: the state of the art. Ind. Eng. Chem. Res. 53, 15020–15040.
Canudas de Wit, C., Olsson, H., Åström, K.J., Lischinsky, P., 1995. A new model for control of systems with friction. IEEE Trans. Automat. Control 40, 419–425.
Choudhury, M.A.A.S., Shah, S.L., Thornhill, N.F., 2008. Diagnosis of Process Nonlinearities and Valve Stiction: Data Driven Approaches. Springer-Verlag, Berlin, Germany.
Choudhury, M.A.A.S., Shah, S.L., Thornhill, N.F., Shook, D.S., 2006. Automatic detection and quantification of stiction in control valves. Cont. Eng. Pract. 14, 1395–1412.
Choudhury, M.A.A.S., Thornhill, N.F., Shah, S.L., 2005. Modelling valve stiction. Cont. Eng. Pract. 13, 641–658.
Coughanowr, D.R., LeBlanc, S.E., 2009. Process Systems Analysis and Control. McGraw-Hill, Boston, MA.
Cuadros, M.A.d.S.L., Munaro, C.J., Munareto, S., 2012. Novel model-free approach for stiction compensation in control valves. Ind. Eng. Chem. Res. 51, 8465–8476.
Durand, H., Christofides, P.D., 2016. Actuator stiction compensation via model predictive control for nonlinear processes. AIChE J. 62, 2004–2023.
Durand, H., Ellis, M., Christofides, P.D., 2014. Integrated design of control actuator layer and economic model predictive control for nonlinear processes. Ind. Eng. Chem. Res. 53, 20000–20012.
Durand, H., Ellis, M., Christofides, P.D., 2016. Economic model predictive control designs for input rate-of-change constraint handling and guaranteed economic performance. Comput. Chem. Eng. 92, 18–36.
Ellis, M., Durand, H., Christofides, P.D., 2014. A tutorial review of economic model predictive control methods. J. Process Control 24, 1156–1178.
Ellis, M., Zhang, J., Liu, J., Christofides, P.D., 2014. Robust moving horizon estimation based output feedback economic model predictive control. Syst. Control Lett. 68, 101–109.
Garcia, C., 2008. Comparison of friction models applied to a control valve. Cont. Eng. Pract. 16, 1231–1243.

Hägglund, T., 2002. A friction compensator for pneumatic control valves. J. Process Control 12, 897–904.
He, Q.P., Wang, J., Pottmann, M., Qin, S.J., 2007. A curve fitting method for detecting valve stiction in oscillating control loops. Ind. Eng. Chem. Res. 46, 4549–4560.
Heidarinejad, M., Liu, J., Christofides, P.D., 2012. Economic model predictive control of nonlinear process systems using Lyapunov techniques. AIChE J. 58, 855–870.
Horch, A., 1999. A simple method for detection of stiction in control valves. Control Eng. Pract. 7, 1221–1231.
Huang, R., Biegler, L.T., Harinath, E., 2012. Robust stability of economically oriented infinite horizon NMPC that include cyclic processes. J. Process Control 22, 51–59.
Ivan, L.Z.X., Lakshminarayanan, S., 2009. A new unified approach to valve stiction quantification and compensation. Ind. Eng. Chem. Res. 48, 3474–3483.
Jelali, M., 2008. Estimation of valve stiction in control loops using separable least--squares and global search algorithms. J. Process Control 18, 632–642.
Jelali, M., Huang, B. (Eds.), 2010. Detection and Diagnosis of Stiction in Control Loops: State of the Art and Advanced Methods. Springer-Verlag, London, England.
Kano, M., Maruta, H., Kugemoto, H., Shimizu, K., 2004. Practical model and detection algorithm for valve stiction. In: Proceedings of the IFAC Symposium on Dynamics and Control of Process Systems. Cambridge, MA, pp. 859–864.
Ljung, L., 1999. System Identification: Theory for the User. Prentice Hall PTR, Upper Saddle River, NJ.
Mohammad, M.A., Huang, B., 2012. Compensation of control valve stiction through controller tuning. J. Process Control 22, 1800–1819.
Munaro, C.J., de Castro, G.B., da Silva, F.A., Angarita, O.F.B., Cypriano, M.V.G., 2016. Reducing wear of sticky pneumatic control valves using compensation pulses with variable amplitude. In: Proceedings of the 11th IFAC Symposium on Dynamics and Control of Process Systems, including Biosystems. Trondheim, Norway, pp. 389–393.
Ogunnaike, B.A., Ray, W.H., 1994. Process Dynamics, Modeling, and Control. Oxford University Press, New York, NY.
Özgülşen, F., Adomaitis, R.A., Çinar, A., 1992. A numerical method for determining optimal parameter values in forced periodic operation. Chem. Eng. Sci. 47, 605–613.
Paduart, J., Lauwers, L., Swevers, J., Smolders, K., Schoukens, J., Pintelon, R., 2010. Identification of nonlinear systems using polynomial nonlinear state space models. Automatica 46, 647–656.
Qin, S.J., Badgwell, T.A., 2003. A survey of industrial model predictive control technology. Cont. Eng. Pract. 11, 733–764.
Rawlings, J.B., Angeli, D., Bates, C.N., 2012. Fundamentals of economic model predictive control. In: Proceedings of the 51st IEEE Conference on Decision and Control. Maui, Hawaii, pp. 3851–3861.
Riggs, J.B., 1999. Chemical Process Control. Ferret Publishing, Lubbock, TX.
Singhal, A., Salsbury, T.I., 2005. A simple method for detecting valve stiction in oscillating control loops. J. Process Control 15, 371–382.
Srinivasan, R., Rengaswamy, R., 2005. Stiction compensation in process control loops: a framework for integrating stiction measure and compensation. Ind. Eng. Chem. Res. 44, 9164–9174.
Srinivasan, R., Rengaswamy, R., 2008. Approaches for efficient stiction compensation in process control valves. Comput. Chem. Eng. 32, 218–229.
Srinivasan, R., Rengaswamy, R., Miller, R., 2005a. Control loop performance assessment. 1. A qualitative approach for stiction diagnosis. Ind. Eng. Chem. Res. 44, 6708–6718.
Srinivasan, R., Rengaswamy, R., Narasimhan, S., Miller, R., 2005b. Control loop performance assessment. 2. Hammerstein model approach for stiction diagnosis. Ind. Eng. Chem. Res. 44, 6719–6728.
Thornhill, N.F., Horch, A., 2007. Advances and new directions in plant-wide disturbance detection and diagnosis. Cont. Eng. Pract. 15, 1196–1206.
Van Overschee, P., De Moor, B.L., 1996. Subspace Identification for Linear Systems: Theory-Implementation-Applications. Kluwer Academic Publishers, Norwell, MA.
Wächter, A., Biegler, L.T., 2006. On the implementation of an interior-point filter line-search algorithm for large-scale nonlinear programming. Math. Program. 106, 25–57.
Wang, J., 2013. Closed-loop compensation method for oscillations caused by control valve stiction. Ind. Eng. Chem. Res. 52, 13006–13019.
Zabiri, H., Samyudia, Y., 2006. A hybrid formulation and design of model predictive control for systems under actuator saturation and backlash. J. Process Control 16, 693–709.